Metasomatic alterations at mafic-ultramafic contacts in Valmalenco (Rhetic Alps, N-Italy)

Autor(en): **Puschnig, André R.**

Objekttyp: **Article**

Zeitschrift: **Schweizerische mineralogische und petrographische Mitteilungen = Bulletin suisse de minéralogie et pétrographie**

Band (Jahr): **82 (2002)**

Heft 3

PDF erstellt am: **09.08.2024**

Persistenter Link: https://doi.org/10.5169/seals-62378

SCHWEIZ. MINERAL. PETROGR. MITT. 82, 515–536, 2002

Dedicated to Prof. Dr. Volkmar Trommsdorff on his 65th anniversary

Metasomatic alterations at mafic-ultramafic contacts in Valmalenco (Rhetic Alps, N-Italy)

by *André R. Puschnig*[1]

Abstract

Effects of oceanic and Alpine alterations have been studied at contacts between basic and ultrabasic rocks in Valmalenco (Rhetic Alps, N-Italy). Metamorphosed altered basalts, so-called metarodingites, consist of a paragenesis of grossular + vesuvianite + chlorite ± diopside ± epidote ± calcite. The mass flux of the rodingitization has been quantified: The rodingites are significantly enriched in calcium (up to 21.5 g CaO per 100 g parent rock), and depleted in sodium (4.5 g Na_2O per 100 g parent rock) and silica (14.4 g SiO_2 per 100 g parent rock) with respect to the unaltered precursor. The enrichment of calcium (rodingitization) was contemporaneous with the serpentinization of ultramafic rocks (breakdown of Ca-bearing orthopyroxene and clinopyroxene) and is interpreted as infiltration of Ca-rich aqueous solutions at an oceanic stage. Elements such as Ti, Zr and V and rare earth elements were not mobilized during oceanic metasomatism and preserve their T-MORB character.
The rodingites show an irregular rim consisting predominantly of chlorite. These rims are called blackwalls and developed during Alpine overprint. They are significantly enriched in magnesium (19.3 g MgO per 100 g parent rock) and depleted in calcium (26.8 g CaO per 100 g parent rock) with respect to the rodingite. The blackwall formation is interpreted as a diffusive process.
The $^{87}Sr/^{86}Sr$ isotopic ratio of the metarodingites is higher than that of the unaltered precursor and lies between the typical values of MOR basalts and Jurassic seawater. This change is interpreted as resulting from strong interaction with seawater.

Keywords: rodingitization, serpentinization, blackwall formation, rare earth elements, Gresens diagram, Sr isotopes.

Zusammenfassung

Effekte von ozeanischen und alpinen Alterationen wurden im Valmalenco (Rhätische Alpen, Norditalien) an Kontakten zwischen basischen und ultrabasischen Gesteinen studiert. Metamorphe alterierte Basalte, sogenannte Rodingite, bestehen dabei aus der Paragenese Grossular + Vesuvian + Chlorit ± Diopsid ± Epidot ± Calcit. Der Massenfluss der Rodingitisierung wurde quantifiziert: Die Rodingite sind im Vergleich zum nicht-alterierten Ausgangsgestein stark an Calcium angereichert (bis 21.5 g CaO auf 100 g Wirtsgestein) und stark an Natrium (bis 4.5 g Na_2O auf 100 g Wirtsgestein) und Silizium (bis 14.4 g SiO_2 auf 100 g Wirtsgestein) abgereichert. Die Zunahme von Calcium lief gleichzeitig mit der Serpentinisierung der ultramafischen Gesteine ab (Zerfall von Ca-führendem Orthopyroxen und Clinopyroxen) und wird als Infiltration von Ca-führenden wässrigen Lösungen in einem ozeanischen Milieu betrachtet. Elemente wie Ti, Zr und V sowie die Seltenen Erde Elemente wurden durch diese ozeanische Metasomatose nicht mobilisert und behalten ihren T-MORB-Charakter.
Die Rodingite weisen einen unregelmässigen Reaktionsrand auf, der hauptsächlich aus Chlorit besteht. Diese Ränder werden als "Blackwalls" bezeichnet, und entstehen während alpiner Überprägung. Sie sind im Vergleich zum Rodingit an Magnesium angereichert (bis 19.3 g MgO auf 100 g Wirtsgestein) und an Calcium abgereichert (bis 26.8 g CaO auf 100 g Wirtsgestein). Die Bildung des "Blackwalls" wird als diffusiver Prozess betrachtet.
Das $^{87}Sr/^{86}Sr$ -Isotopenverhältnis der Metarodingite ist höher als das des nicht-alterierten Ausgangsgesteins und liegt zwischen den typischen Werten von MOR-Basalten und dem Wert von Jurassischem Meerwasser. Diese Änderung wird als Interaktion mit Meerwasser interpretiert.

[1] Institut für Mineralogie und Petrographie, ETH-Zentrum, CH-8092 Zürich.
Present address: Naturhistorisches Museum Basel, Augustinergasse 2, CH-4001 Basel. <andre.puschnig@bs.ch>

1. Introduction

Chemical changes of oceanic rocks, like serpentinization, chloritization (a Mg–Ca metasomatism) and spilitization (a Na metasomatism), are reported from the ocean floor as result of fluid-rock interaction. Rather subordinate known from the ocean floor is rodingitization, that have been found and studied by HONNOREZ and KIRST (1975). Rodingites are Ca enriched and Si depleted rocks and occur in association with serpentinized ultramafic rocks. In many cases they develop as result of hydrothermal alteration and element exchange between ultramafic and mafic rocks in an oceanic setting (e.g. COLEMAN, 1967, 1977; HONNOREZ and KIRST, 1975). Studies of this rodingitization process on the ocean floor are rare. This is related to the difficulty of extensive sampling on the ocean floor. Additionally, direct observations of large rock sections to quantify the results of rodingitization are not possible.

In contrast, ophiolites with their easy access and large outcrop areas provide detailed information on effects of hydrothermal processes on the ancient ocean floor, e.g. the rodingitization. However, studies in these units are often complicated by metamorphic overprint due to orogenic processes.

In ophiolites of the Alps different occurrences of rodingites have been described for Liguria (BARRIGA and FYFE, 1983; SCAMBELLURI and RAMPONE, 1999), the Central Alps (KEUSEN, 1972; EVANS et al., 1981), and the eastern Central Alps (RÖSLI, 1988). Some chemical studies exist (e.g. KEUSEN 1972; RÖSLI 1988; SCAMBELLURI and RAMPONE 1999), but the behaviour of main, trace, rare elements and Sr isotopes has not been studied in detail at one section.

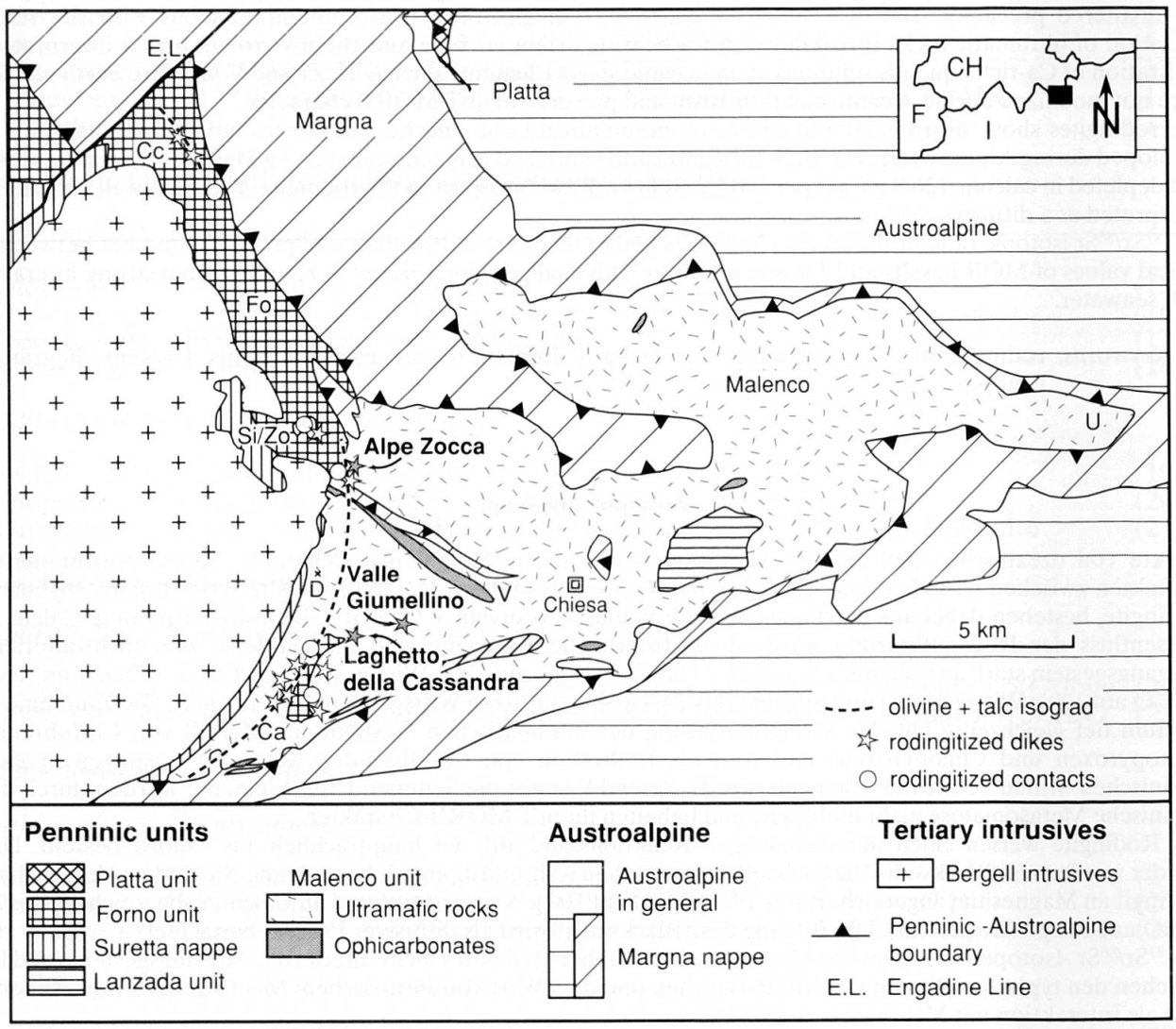

Fig. 1 Geological-tectonic map of the eastern border of the Bergell intrusion. Sample locations of the alteration zones within the Forno-Malenco unit are indicated (with filled stars). Ca—Cassandra area, Cc—Cavloc area, D—Monte Disgrazia, Fo—Forno area, Si/Zo—Sissone/Zocca area, U—Pass d'Ur, V—Passo Ventina. The contact metamorphic olivine + talc isograd is after TROMMSDORFF and NIEVERGELT (1983) and TROMMSDORFF and CONNOLLY (1996).

In the Forno-Malenco unit in the eastern Central Alps, mafic dikes and mafic bodies in direct contact to ultramafic rocks are transformed to calc-silicate rocks (rodingites, PUSCHNIG, 2000). Additionally, all these contacts show a small chlorite- and amphibole-rich zone (blackwalls).

The aims of this paper are: (i) to give a petrographic description of rodingites and blackwalls of the Forno unit, (ii) to estimate whole rock gains and losses of main elements of the altered rocks (rodingites and blackwalls) and to quantify the effects of the alteration by mass balance calculation after GRESENS (1967), and (iii) to evaluate the behaviour of trace and rare earth elements (REE) as well as the behaviour of Sr isotopes during rodingitization.

2. Geological setting

The studied area is situated in a nappe edifice that comprises three major tectonic complexes characterizing the Penninic-Austroalpine boundary in southeastern Switzerland and Northern Italy (Fig. 1). Alpine thrusting resulted in a nappe pile involving from top to bottom and east to west:

(1) The Lower Austroalpine *Bernina* and *Margna nappes*, consisting of crystalline basement and Permo-Mesozoic cover, represent the distal part of the Adriatic continental margin (MONTRASIO and TROMMSDORFF, 1983; WEISSERT and BERNOULLI, 1985).

(2) The South Penninic *Malenco* and *Forno units* are a part of the Tethys ocean. The Malenco ultramafic body is one of the largest ultramafic masses in the Alps (130 km^2) dominated by variably serpentinized ultramafic rocks. The exhumation on the ocean floor is documented by a penetrative serpentinization of the Malenco ultramafics, supported by marine signatures of stable isotopes in serpentine minerals (BURKHARD and O'NEIL, 1988), and by ophicarbonates (TROMMSDORFF and EVANS, 1977; POZZORINI and FRÜH-GREEN, 1996).

The *Forno unit* is an ocean floor sequence of metabasaltic rocks with locally preserved pillow lavas and pillow breccias (MONTRASIO, 1973) and a metasedimentary cover. Intrusive relationships between the Forno mafics and the ultramafic rocks of the Malenco unit are documented by basaltic dikes crosscutting the Malenco ultramafic rocks (stars on Fig. 1; TROMMSDORFF et al., 1993; ULRICH and BORSIEN, 1996; PUSCHNIG, 1998, 2000). The dikes have subsequently been rodingitized. Major, trace and REE geochemical data (GAUTSCHI, 1980; PUSCHNIG, 1998, 2000) as well as the Pb-isotopic signatures of the mafic rocks (PERETTI and KÖPPEL, 1986) reveal a MORB character. The sediments consisting of metamorphosed radiolarian cherts, Calpionella limestones (calc-silicates and calcite marbles), metapelites and meta-arkoses with pelite and carbonate intercalations are assumed to be of Mid(?)–Late Jurassic to Early Cretaceous age (WEISSERT and BERNOULLI, 1985).

(3) The Middle Penninic *Suretta nappe*, derived from the Briançonnais domain (SCHMID et al., 1990), is composed of a crystalline basement and a Permo-Mesozoic cover.

The Alpine regional metamorphism increases from north to south, reaching epidote-amphibolite facies conditions in the studied area (EVANS and TROMMSDORFF, 1970; GAUTSCHI, 1980; HERMANN, 1997). Radiometric ages yield a Late Cretaceous age (JÄGER, 1973; FREY et al., 1974; PHILIPP, 1982; DEUTSCH, 1983; HANDY et al., 1996; HERMANN, 1997) for the Alpine metamorphic peak. The nappe pile was locally intruded by the Oligocene calc-alkaline Bergell (Bregaglia) intrusion. These intrusives metamorphosed the surrounding rocks of the Malenco-Forno unit, the Suretta and Margna nappe, resulting in a 1.5 to 2 km wide contact aureole (TROMMSDORFF and EVANS, 1972; TROMMSDORFF and NIEVERGELT, 1983; PFIFFNER and WEISS, 1994; TROMMSDORFF and CONNOLLY, 1996).

3. Metasomatic alteration

Rodingites and blackwalls at three different localities of the Forno-Malenco unit have been studied in detail. The first locality is situated 250 m northeast of Laghetto della Cassandra (Fig. 1), the second locality 2 km north of Rif. Bosio in Valle Giumellino and the third locality at Alpe Zocca southeast of Chiareggio (described by BORSIEN, 1995). They are representative, as they show the important and common alteration zones. All studied metarodingite-serpentinite contacts lie outside of the contact metamorphic olivine + talc isograd (Fig. 1) and have a regional metamorphic epidote-amphibolite facies overprint.

3.1. FIELD OCCURRENCE AND SAMPLE DESCRIPTION

The metarodingites crop out as dikelets within serpentinized ultramafic rocks, and are on a meter scale often associated with metapyroxenites. In all three areas, the rocks are affected by the main Alpine deformation phase D_1, that produced the main foliation S_1 in the study area. This phase D_1

Table 1 Summary of the parageneses in rodingites, blackwalls and serpentinites at different stages from a pre-oceanic stage to Late Alpine overprint. Am—amphibole, atg—antigorite, cal—calcite, chl—chlorite, cpx—clinopyroxene, ctl—chrsyotile, di—diopside, ep— epidote, grs—grossular, ilm—ilmenite, mag—magnetite, ol—olivine, pl—plagioclase, tr—tremolite, ttn—titanite, ves—vesuvianite.

Observations	**prekinematic**	**prekinematic**	**synkinematic**	**postkinematic**
Interpretation	**magmatic and pre-oceanic stage**	**oceanic metamorphism (lower greenschist facies)**	**Alpine regional metamorphism (epidote-amphibolite facies)**	**Oligocene contact metamorphism (amphibolite facies)**
basalt rodingite	pl + ol + cpx ?	grs_1 + ves_1 + chl_1 ± di ± ep ± cal		
metarodingite			grs_2 + ves_2 + chl_2 ± cal	am
amphibole blackwall	cpx?	di ± ep	am_1 ± chl ± grs ± cal ± ttn	am_2
chlorite blackwall		di ± cal	chl ± ilm ± ttn	tr + cal
serpentinite	cpx	ctl?	atg + ol + mag + di + chl	tr + cal

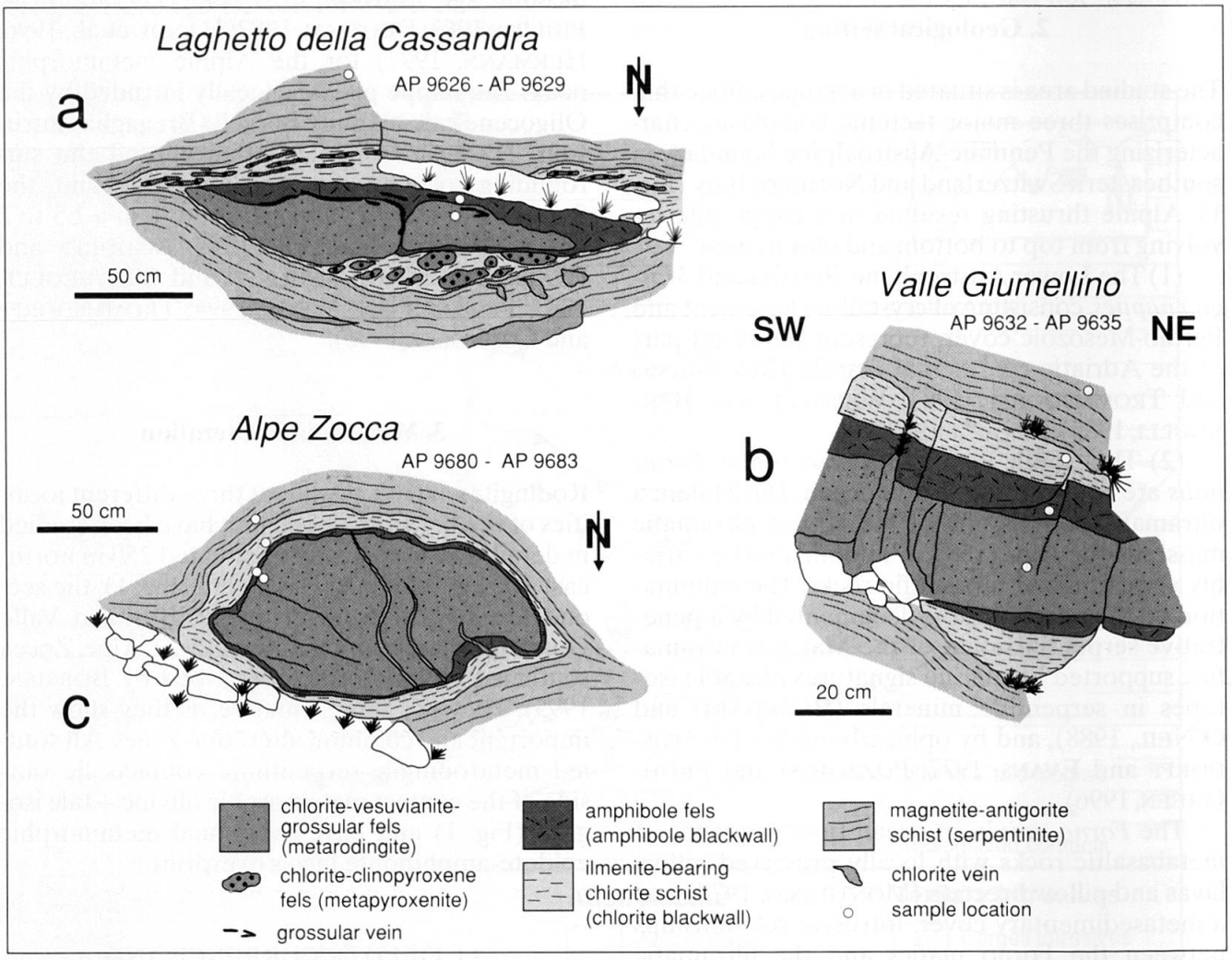

Fig. 2 Studied metarodingite boudins at (a) Laghetto della Cassandra (Swiss grid coordinates 779.540/124.730), (b) Valle Giumellino (Swiss grid coordinates 781.090/125.600) and (c) Alpe Zocca (Swiss grid coordinates 779.550/129.500).

is the result of an Upper Cretaceous nappe stacking in the South Penninic-Austroalpine realm (FROITZHEIM et al., 1994). Refolding of the nappe stacking (D_2, D_4 and D_6, PUSCHNIG, 1996) and extensional structures (D_3) affecting the nappe pile, as well as local deformations (D_5, D_7, D_8) due to the emplacement of the Bergell pluton do not affect macroscopically the studied contact zones.

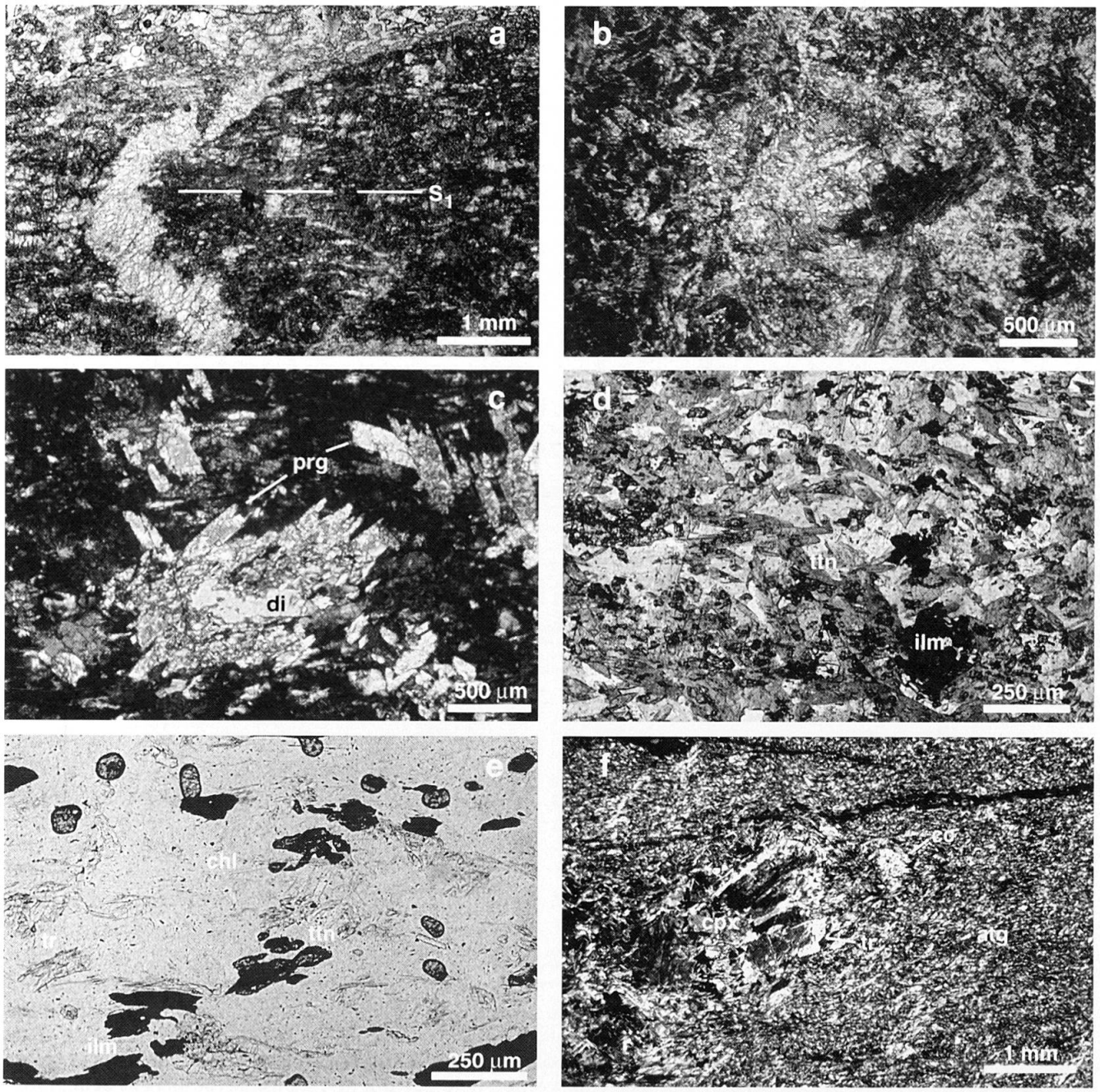

Fig. 3 Microscopic observations in the alteration zones. **(a)** Metarodingite: A vein of vesuvianite is folded and recrystallized parallel the fold axial plane, that corresponds to S_1. Dynamic recrystallization of grossular, vesuvianite, chlorite in S_1 (AP 9626; plane polarized light). **(b)** Metarodingite with preserved magmatic texture (?): In an intersertal texture grossular and vesuvianite form ledges pseudomorphically after plagioclase. The ancient probably glassy matrix is represented by chlorite and vesuvianite (AP 9680; plane polarized light). **(c)** Metarodingite: Subordinate diopside (di) is postkinematically overgrown by pargasites (prg; AP 9626; crossed polarized light). **(d)** Amphibole blackwall: Pargasitic hornblende in a matrix of chlorite, titanite (ttn) and ilmenite (ilm; AP 9633; plane polarized light). **(e)** Chlorite blackwall: Chlorite schist (chl) with titanite (ttn), ilmenite (ilm) and tremolite (tr; AP 9634; plane polarized light). **(f)** Serpentinite: Antigorite (atg) with prekinematic clinopyroxene (cpx), which is retrogressed to tremolite (tr) and calcite (cc; AP 9629, crossed polarized light).

The structural relationships between the different lithological units is summarized in Fig. 2. The surrounding serpentinite displays a pervasive foliation S_1 that is cut by chlorite veins. The metarodingites and metapyroxenites were boundinaged parallel to the serpentinite foliation during deformation D_1. Within the metarodingites fine-grained calc-silicate minerals are macroscopically not deformed and provide the opportunity to recognize pre-Alpine textures and mineral relics. The metarodingites display centimeter-wide reaction zones at the contact to the country rock serpenti-

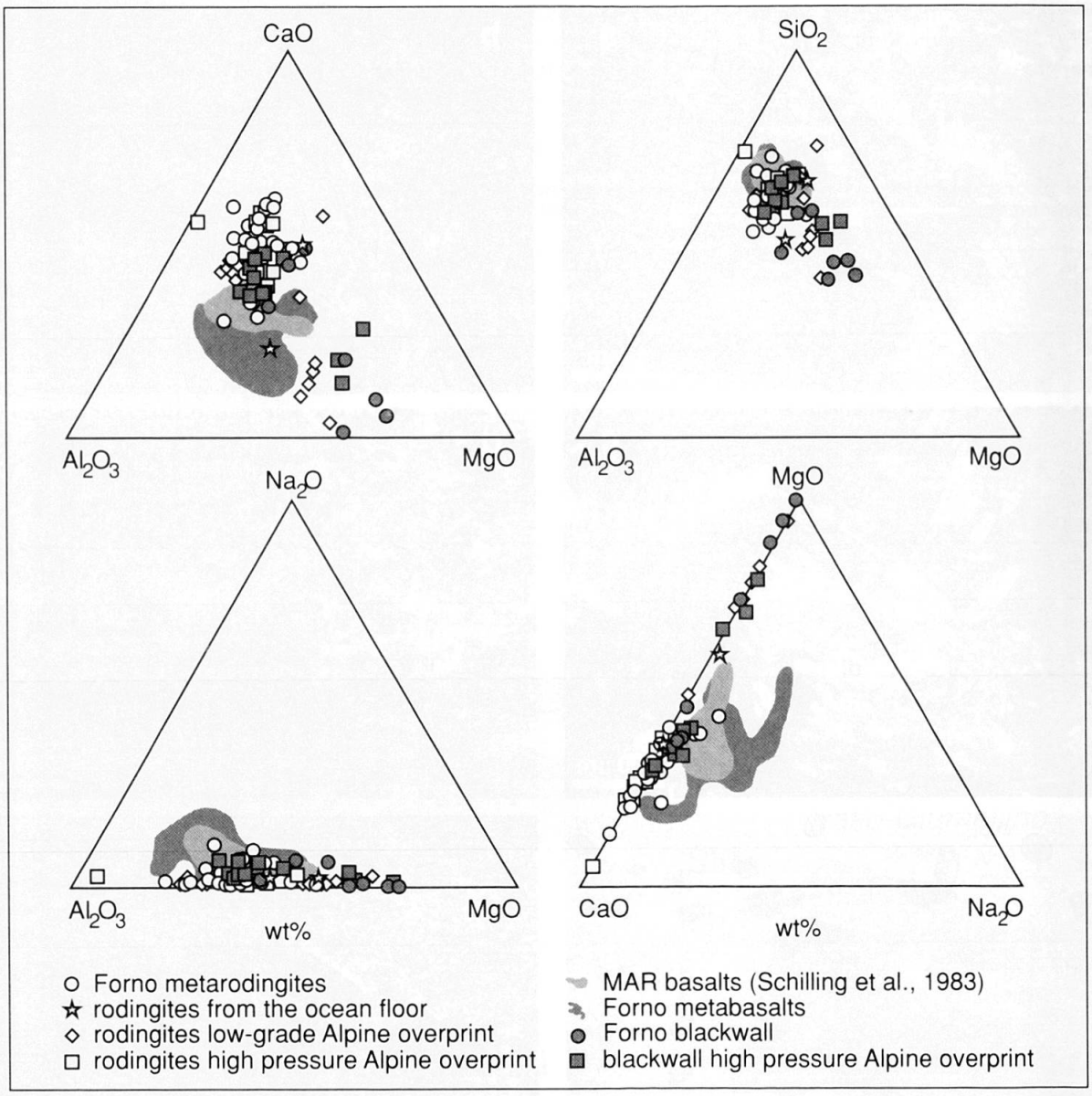

Fig. 4 The effect of alteration on Forno metabasalts and Forno metarodingites for some important elements like SiO_2, Al_2O_3, CaO, MgO, Na_2O in wt%. Bulk-rock chemistry values are shown for Forno metabasalts (own data; GAUTSCHI, 1980; KUBLI, 1983; DIETHELM, 1984; GIERÉ, 1985; BORSIEN, 1995) and for Forno metarodingites and blackwalls (own data; BORSIEN, 1995; PAGLIA, 1996). The composition field of fresh MAR basalts (SCHILLING et al., 1983) and rodingites with low-grade Alpine overprint (RÖSLI, 1988), rodingites with high pressure Alpine overprint (EVANS et al., 1981; WIDMER, 1996; PFIFFNER, 1999) and blackwalls with high pressure Alpine overprint (PFIFFNER, 1999) are given for comparison.

nite. The inner part of this zone is made predominantly of amphibole, the outer part predominantly of chlorite. These zones are called amphibole and chlorite blackwall, respectively.

In all localities profiles were sampled from the core of the metarodingite to the country rock serpentinite. Four zones have been distinguished (see Fig. 2 and Table 1):

(a) Metarodingite zone: the core of the dike consists of micro-domains (up to 2 mm) of an equigranular assemblage of grossular, vesuvianite, ± chlorite, ± calcite, ± diopside surrounded by synkinematic grossular, vesuvianite, chlorite, calcite, titanite. At Laghetto della Cassandra garnet and vesuvianite veins are preserved in the central part. The outer part of the metarodingite zone is folded (Fig. 3a). At Alpe Zocca probably a magmatic texture is preserved in the central part: In an intersertal texture grossular and chlorite form long ledges, and fine-grained chlorite and vesuvianite the matrix (Fig. 3b). Subordinate diopside is partially overgrown by pargasite (Fig. 3c).

(b) Amphibole blackwall zone: the inner part of the dike rim develops gradually from the rodingite. It consists of actinolitic hornblende, chlorite, calcite, ± titanite, ± grossular. Diopside and epi-

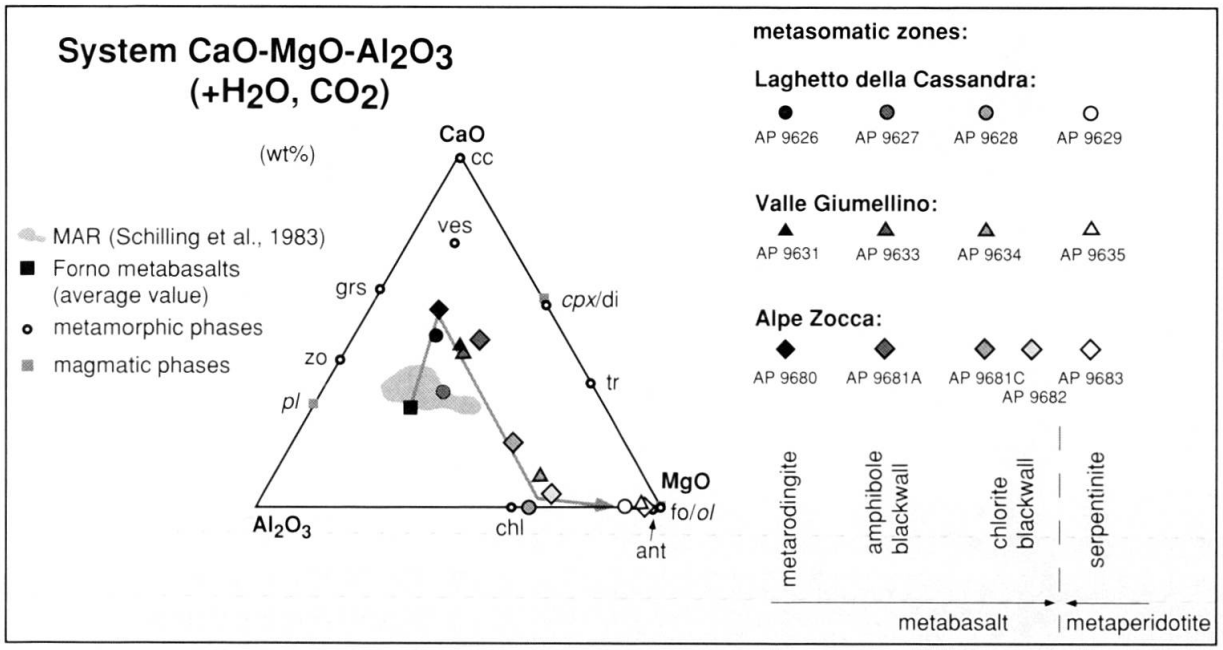

Fig. 5 Al_2O_3–CaO–MgO diagram showing the effect of rodingitization and blackwall formation at the studied localities in wt%. Bulk-rock chemistry values are shown for metarodingites, the blackwalls and the serpentinites. The composition field of fresh dredged MAR basalt (SCHILLING et al., 1983) and an average composition of Forno metabasalts are given for comparison.

dote occur as relics only, and actinolitic hornblende is locally overgrown by pargasitic hornblende (Fig. 3d). Locally garnet veins are preserved or are replaced by hornblende.

(c) Chlorite blackwall zone: the outer part of the dike rim consists of a synkinematic assemblage of chlorite and ilmenite, overgrown by idiomorphic tremolite and calcite (Fig. 3e). Prekinematic relics are diopside and calcite. This blackwall has a sharp contact to the serpentinite.

(d) The serpentinite zone: the wall rock, consisting of synkinematic antigorite, magnetite and ± olivine. Relics of xenomorphic clinopyroxenes are partially overgrown by postkinematic tremolite and calcite (Laghetto della Cassandra, Fig. 3f).

3.2. WHOLE ROCK COMPOSITION

In Figure 4 the chemical composition of the Forno metabasalts is compared with fresh dredged basalts from the Mid-Atlantic Ridge (MAR, SCHILLING et al., 1983). With the exception of Na_2O, the variation of the MgO/Al_2O_3 ratio and the rather constant SiO_2 content of the Forno metabasalts overlaps with that of the MAR basalts. This most probably reflects a tholeiitic differentiation trend. The increase of Na_2O from 0.87 to 5.02 wt% indicates partial spilitization of the Forno metabasalts.

The Forno rodingites display an enrichment in CaO, depletion in SiO_2 and Na_2O compared with the MAR basalts and Forno metabasalts (Fig. 4, Table 2). Rodingites from the ocean floor (HONNOREZ and KIRST, 1975) and rodingites with a high pressure Alpine overprint (EVANS et al., 1981; WIDMER, 1996; PFIFFNER, 1999) for comparison show the same trends. Rodingites with a low-grade Alpine overprint (prehnite-pumpellyite facies, RÖSLI, 1988) are enriched in MgO from 6.55 to 25.34 wt%.

The Forno blackwalls display a strong enrichment of MgO and loss of CaO and SiO_2 (Fig. 4). Blackwalls with a high pressure overprint (PFIFFNER, 1999) show the same enrichment/depletion trends as the Forno blackwalls.

In Figure 5 the chemical compositions of the blackwalls from the three studied localities in Valmalenco are compared to MAR basalts (SCHILLING et al., 1983) and an average value of Forno metabasalts. The amphibole blackwalls display a decrease of CaO and a slight increase of MgO. The chlorite blackwall has a strong loss of CaO (compared with the amphibole blackwall) and a strong MgO increase. The chlorite blackwall exhibits the same MgO/SiO_2 ratio as the neighbouring serpentinite and can only be distinguished from the serpentinite by the higher Al_2O_3 content.

Increasing rodingitization (documented by an increase in CaO) decreases the contents of SiO_2 and Na_2O (Fig. 6). Most of the metarodingites are depleted in Sr with respect to the metabasalts. Some samples of the metabasalts and metarodin-

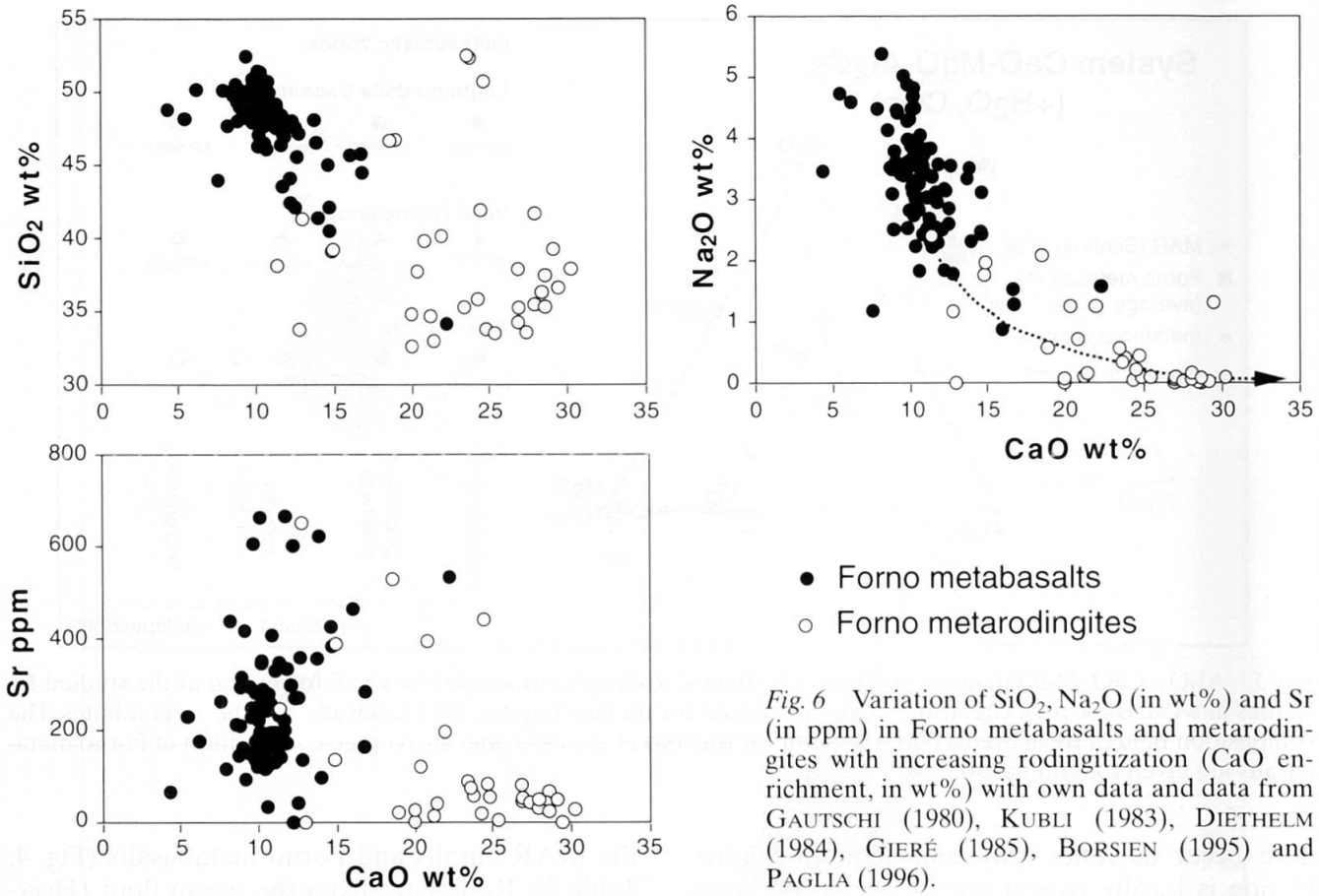

Fig. 6 Variation of SiO_2, Na_2O (in wt%) and Sr (in ppm) in Forno metabasalts and metarodingites with increasing rodingitization (CaO enrichment, in wt%) with own data and data from GAUTSCHI (1980), KUBLI (1983), DIETHELM (1984), GIERÉ (1985), BORSIEN (1995) and PAGLIA (1996).

gites however display an enrichment of Sr up to 650 ppm. This affects all samples with epidote in their assemblage. The high field strength elements Ti, Zr, as well as Y and V of the rodingites display a good correlation and overlap with the area defined by the Forno metabasalts (Fig. 7).

The Forno metarodingites from the Cavloc, Cassandra and Sissone/Zocca area (Fig. 1) have a relatively flat chondrite-normalized REE pattern (Fig. 8). The Cavloc metarodingites display a slight enrichment of LREE with respect to the HREE. The $(La/Yb)_N$ ratio shows a range from 1.08 to 1.80 and a $(La/Sm)_N$ ratio from 0.70 to 0.95 (Table 3). The REE patterns of these metarodingites are slightly higher than the adjacent Forno metabasalts, which have the same overall characteristics. The Cassandra metarodingites display a stronger enrichment of LREE to HREE with respect to the Cavloc metarodingites. The $(La/Yb)_N$ and $(La/Sm)_N$ ratios range from 1.42 to 2.96 and from 0.86 to 1.65, respectively. The REE patterns are similar to the adjacent metabasalts, but are slightly higher, show a greater variation and have higher LREE contents. The Sissone/Zocca metarodingites show also a higher LREE content with respect to the HREE. The $(La/Yb)_N$ ratio ranges from 1.27 to 3.32, the $(La/Sm)_N$ ratio from 0.92 to 2.08. The REE patterns are similar to that of the adjacent metabasalts. The REE contents increase with increasing differentiation, as documented by Yb_N (Fig. 8d).

The amphibole and chlorite blackwalls of the studied localities Giumellino and Alpe Zocca display identical or slightly higher values for immobile elements such as Ti and Zr (Table 2) compared with the metarodingites. For the same elements the serpentinite shows distinctly lower values for both metarodingites and blackwalls. A different behaviour is observed for compatible elements such as Ni and Cr, which generally do not vary across the alteration zones from metarodingite to the chlorite blackwall. In the serpentinite, these elements are distinctly enriched. For localities Giumellino and Alpe Zocca there is a gap of the individual contents of trace elements from the basaltic to the ultramafic protolith. For locality Cassandra the gap is blurred.

3.3. MASS BALANCE CALCULATIONS

Rodingitization and serpentinization

The process of rodingitization has to be considered together with the process of serpentinization to deduce the possible relation of contrasting element behaviour. In order to apply the composi-

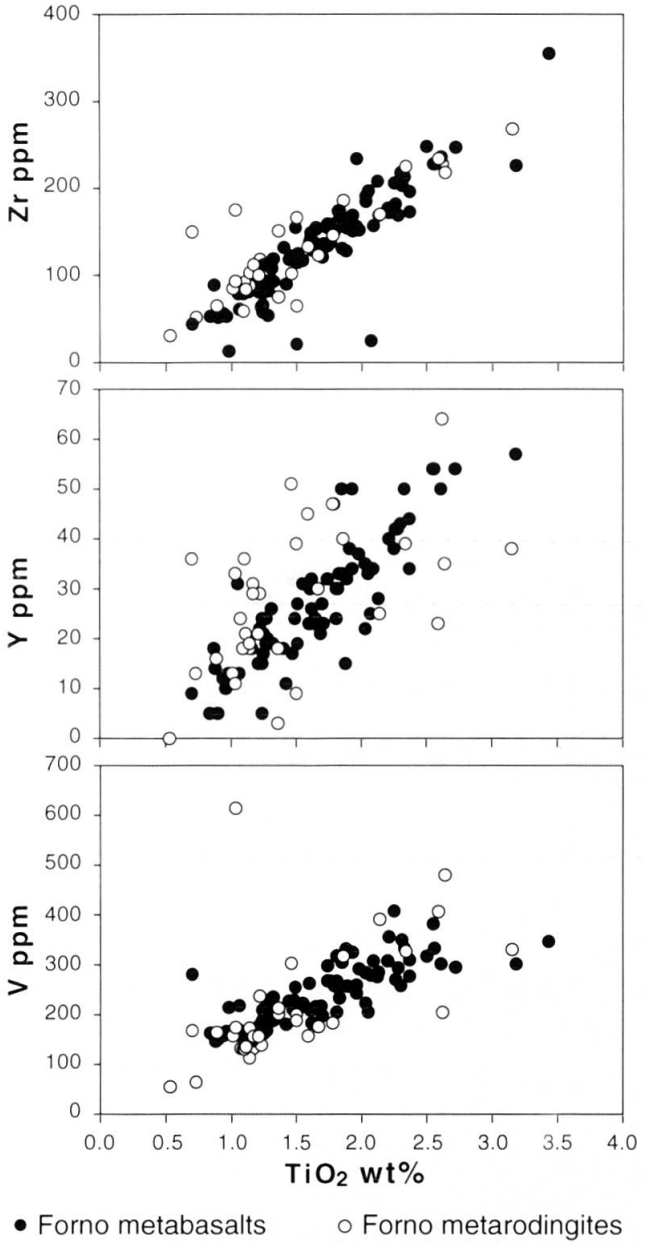

Fig. 7 Variation of incompatible elements Zr, Y, and V (ppm) in Forno matabasalts and metarodingites with TiO_2 (wt%) with own data and data from GAUTSCHI (1980), KUBLI (1983), DIETHELM (1984), GIERÉ (1985), BORSIEN (1995) and PAGLIA (1996).

tion-volume relationship after GRESENS (1967), it is important to identify a possible protolith (metabasalt, peridotite) whose composition is essentially unchanged. However, the bulk-rock composition of a basalt changes with differentiation and therefore metabasalts close to the respective locality and with a composition similar to the metarodingites have been chosen as protolith, assuming a similar degree of differentiation as the metarodingites. For this reason samples AP 9623 (Laghetto della Cassandra), AP 9624 (Valle Giumellino) and 93-G 28 (from BORSIEN, 1995; Alpe Zocca) have been taken for comparison (Table 2).

Serpentinites in contact with the alteration zones are harzburgitic in composition, as can be demonstrated by samples AP 9635 and AP 9683 (Table 2). These serpentinites have been recalculated on a H_2O-free basis and compared with non-serpentinized Malenco peridotites (Table 1, L-UM 216 and L-UM 401, MÜNTENER and HERMANN, 1996; MÜNTENER, 1997). The H_2O content in these two samples is caused by minor pre-Alpine amphibole and chlorite. The samples AP 9635 and AP 9683 are in acceptable agreement with the peridotite L-UM 401 based upon MgO, Al_2O_3 and TiO_2. The same holds for AP 9629 compared with L-UM 216.

Serpentinite

Serpentinites from all three localities display for the serpentinization process a constant loss of CaO of 1.7 to 2.0 g per 100 g parent rock over the whole range of volume factors (Fig. 9). The loss of CaO may be explained by the breakdown of clinopyroxene and/or of Ca-bearing orthopyroxene during serpentinization. Additionally, there is a constant gain of the volatiles, documented by the modal predominance of antigorite in the rock containing up to 14 wt% H_2O, growing at the expense of olivine.

For all localities SiO_2 and MgO intercept the zero line of concentration change at volume factors ranging from 1.24 to 1.34. These elements point to a volume increase during serpentinization of 24 to 34%. In minor amounts Al_2O_3 is removed from the localities Giumellino and Zocca by 0.3 to 0.4 g per 100 g parent rock, whereas in the locality Cassandra Al_2O_3 is added by 0.6 g per 100 g parent rock (at a volume factor of 1.3). Due to the problem of the choice of the protolith that fits the serpentinite, these small gains and losses are considered as irrelevant and Al_2O_3 to be immobile.

For TiO_2, Cr_2O_3 and NiO the mobility is in the range of – 0.15 to 0.08 g per 100 g parent rock and these elements can therefore be considered as immobile.

FeO_{tot} is lost in localities Giumellino and Zocca (2 g per 100 g parent rock) and enriched in locality Cassandra (1 g per 100 g parent rock, for a volume factor of 1.3). As there is already a primary variation in the iron content of fresh peridotites of the Malenco unit (MÜNTENER, 1997), gains and losses seem to be reasonable.

Rodingite

In all diagrams of Fig. 10 Na_2O is lost relative to the chosen metabasalt over the entire range of volume factors. In localities Giumellino and Zocca, MgO and Al_2O_3 intercept the zero line at vol-

Table 2 Bulk-rock analyses of rodingites, blackwalls, serpentinites, metabasalts and peridotites (X-Ray fluorescence). Bulk-rock compositions were determined with a sequential spectrometer (Philips PW 1404) at EMPA Dübendorf/Switzerland. The analytical uncertainties are about 1 to 8% (standard deviation 1σ). Metabasalt 93-G 28 is from BORSIEN (1995, Alpe Zocca), and peridotites L-UM 216 and 401 are from MÜNTENER (1997). Cc—Cavloc area, Ca—Cassandra area, Si/Zo—Sissone/Zocca area. Rod—rodingite, Am bl— amphibole blackwall, Chl bl—chlorite blackwall, Serp— Serpentinite, Perid—peridotite, Fo—Forno metabasalt, recalc.—serpentinite recalculated on to a volatile-free basis. Sp. gr.—specific gravity (gravimetric determination). $X_{Mg} = MgO/(MgO + FeO_{tot})$.

sample	AP 9425	AP 9436	AP 9437	AP 9454	AP 9418	AP 9421	AP 9423	AP 9473	AP 9542	AP 9543	AP 9546	AP 9547	AP 9548	AP 9626	AP 9631	AP 9632	AP 9636	AP 9407	AP 9555	AP 9556	AP 9557	AP 9560	AP 9571
	Rod	Rod	Rod	Rod	Rod	Rod	Rod	Rod	Rod	Rod	Rod	Rod	Rod	Rod	Rod	Rod	Rod	Rod	Rod	Rod	Rod	Rod	Rod
area	Cc	Cc	Cc	Cc	Ca	Ca	Ca	Ca	Ca	Ca	Ca	Ca	Ca	Ca	Ca	Ca	Ca	Si/Zo	Si/Zo	Si/Zo	Si/Zo	Si/Zo	Si/Zo
(wt%)																							
SiO_2	33.77	38.11	46.66	39.20	34.66	34.80	37.88	39.09	36.30	39.24	33.77	35.24	34.24	35.26	32.97	32.62	33.57	46.73	41.68	33.49	35.47	41.91	37.90
TiO_2	2.64	3.15	2.14	1.03	2.59	1.36	1.50	1.03	1.36	1.09	1.11	1.21	1.14	1.10	1.59	1.78	1.17	4.24	1.86	1.23	1.07	1.22	0.73
Al_2O_3	21.59	15.56	12.74	17.65	18.59	18.47	10.82	17.94	13.75	10.57	16.80	12.94	16.70	14.88	12.55	11.18	15.30	2.09	15.59	16.35	15.73	14.30	12.63
Fe_2O_3	14.41	15.93	9.99	11.21	12.31	10.38	11.31	11.30	8.53	9.28	9.17	9.93	7.71	11.10	12.29	13.79	7.56	13.07	7.11	9.16	7.78	7.73	6.80
MnO	0.22	0.27	0.2	0.19	0.19	0.25	0.19	0.18	0.14	0.13	0.17	0.21	0.22	0.20	0.25	0.24	0.25	0.32	0.17	0.11	0.15	0.14	0.06
MgO	9.05	10.47	5.53	10.83	6.73	9.16	7.96	10.70	7.80	7.91	8.93	8.41	8.36	8.97	12.25	13.70	8.23	12.46	4.15	10.39	8.40	6.38	7.89
CaO	12.76	11.37	18.54	14.90	21.18	19.93	26.89	14.82	28.40	29.13	24.83	26.94	26.90	23.40	21.40	19.94	27.43	18.89	27.98	25.39	27.96	24.47	30.22
Na_2O	1.17	2.40	2.08	1.96	0.10	0.00	0.00	1.76	0.01	0.02	0.09	0.09	0.05	0.56	0.15	0.07	0.02	0.57	0.16	0.09	0.06	0.21	0.09
K_2O	0.21	0.33	0.03	0.17	0.01	0.00	0.00	0.17	0.00	0.00	0.00	0.00	0.00	0.01	0.00	0.00	0.00	0.06	0.07	0.00	0.00	0.00	0.00
P_2O_5	0.13	0.01	0.13	0.02	0.41	0.14	0.19	0.02	0.25	0.11	0.13	0.13	0.15	0.11	0.17	0.19	0.14	0.01	0.25	0.13	0.11	0.17	0.08
Cr_2O_3	0.03	0.04	0.03	0.03	0.01	0.04	0.02	0.03	0.02	0.04	0.03	0.03	0.03	0.04	0.05	0.04	0.03	0.03	0.03	0.04	0.03	0.03	0.03
NiO_2	0.00	0.01	0.00	0.03	0.00	0.02	0.02	0.03	0.01	0.02	0.02	0.02	0.02	0.03	0.03	0.03	0.02	0.02	0.00	0.02	0.01	0.00	0.03
L.O.I.	3.36	0.68	0.75	1.95	2.68	3.06	1.38	1.17	2.05	1.63	3.48	3.55	3.07	4.73	6.31	6.84	4.50	0.00	0.49	2.44	2.00	2.15	2.58
Σ	99.34	98.33	98.82	99.46	99.46	97.61	98.21	98.24	98.62	99.17	98.53	98.70	98.59	100.39	100.01	100.42	98.22	98.49	99.54	98.34	98.77	98.71	99.04
(ppm)																							
F	441	313	534	222	512	440	662	773	595	502	356	294	673	623	238	133	802	695	1218	237	316	190	530
Ba	38	29	12	<10	33	10	10	106	12	<10	<10	<10	<10	15	<10	<10	<10	43	27	<10	<10	<10	<10
Rb	<8	<8	<8	<8	<8	<8	<8	<8	<8	<8	<8	<8	<8	<8	<8	<8	<8	<8	11	<8	<8	<8	<8
Sr	651	247	529	388	14	<15	81	136	43	49	55	53	46	89	41	27	43	22	49	<15	31	441	28
Pb	<5	<5	<5	<5	<5	<5	<5	<5	<5	12	<5	<5	<5	7	6	6	<5	<5	<5	<5	6	18	<5
Th	<5	<5	<5	<5	<5	<5	<5	<5	<5	<5	<5	<5	<5	<5	<5	<5	<5	<5	<5	<5	<5	<5	<5
U	<10	<10	<10	<10	<10	<10	<10	<10	<10	<10	<10	<10	<10	<10	<10	<10	<10	<10	<10	<10	<10	<10	<10
Nb	<4	<4	<4	12	<4	<4	<4	<4	<4	<4	<4	<4	<4	15	15	16	11	<4	<4	<4	4	8	<4
La	<20	32	<20	<20	<20	<20	<20	<20	<20	<20	<20	<20	<20	<20	<20	<20	<20	60	<20	<20	<20	<20	<20
Ce	36	55	<15	<15	32	<15	23	<15	<15	<15	<15	<15	<15	<15	<15	17	<15	39	25	<15	<15	<15	<15
Nd	28	36	<25	<25	29	<25	<25	<25	<25	<25	<25	<25	<25	<25	<25	<25	<25	38	<25	<25	<25	<25	<25
Y	35	38	25	33	23	3	9	11	18	18	21	21	19	36	45	47	29	13	40	15	24	29	13
Zr	218	268	170	93	234	75	65	175	151	59	84	100	103	92	133	146	112	273	186	64	89	118	52
V	480	331	391	174	407	201	188	614	213	131	135	156	173	130	157	183	156	327	317	139	132	237	64
Cr	198	300	187	212	60	352	151	161	65	318	175	136	189	279	283	353	240	237	87	251	275	265	309
Ni	75	129	70	246	66	234	235	82	116	222	176	172	165	298	282	314	161	195	69	231	150	58	248
Co	89	124	56	86	110	89	97	77	68	101	63	72	51	105	108	116	72	119	42	76	79	56	73
Cu	<3	198	59	43	22	<3	<3	360	3	20	<3	<3	<3	41	8	9	17	50	<3	<3	11	6	26
Zn	66	138	47	70	90	78	44	62	31	55	75	82	80	57	93	92	61	85	27	38	55	55	27
Ga	18	12	14	11	7	8	2	<2	7	8	9	10	9	7	8	8	7	<2	15	8	7	15	5
Sc	62	58	39	38	30	24	22	56	23	3	28	25	21	28	34	38	12	65	30	18	15	18	<2
S	<50	<50	<50	<50	<50	<50	<50	<50	<50	<50	<50	<50	<50	<50	<50	<50	<50	<50	<50	<50	<50	<50	<50
X_{Mg}	0.41	0.42	0.38	0.52	0.38	0.50	0.44	0.51	0.50	0.49	0.52	0.48	0.55	0.47	0.53	0.52	0.55	0.51	0.39	0.56	0.55	0.48	0.56
Sp. gr.														3.20	3.01								

Table 2 continued

sample	AP 9680 Rod	AP 9686 Rod	AP 9687 Rod	AP 9627 Am bl	AP 9628 Chl bl	AP 9633 Am bl	AP 9634 Chl bl	AP 9681A Am bl	AP 9681C Chl bl	AP 9682 Chl bl	AP 9629 Serp	AP 9635 Serp	AP 9683 Serp	AP 9629 recalc.	AP 9635 recalc.	AP 9683 recalc.	L-UM 216 Perid	L-UM 401 Perid	AP 9623 Fo	AP 9624 Fo	93-G 28 Fo	Average Forno basalt
area	Si/Zo	Si/Zo	Si/Zo	Ca	Ca	Ca	Ca	Si/Zo	Si/Zo	Si/Zo	Ca	Ca	Si/Zo						Ca	Ca	Si/Zo	
(wt%)																						
SiO_2	35.31	50.70	52.47	26.46	30.56	32.43	33.38	30.32	29.69	32.15	40.73	41.00	41.41	45.56	45.92	45.62	42.8	43.5	47.05	47.92	47.94	47.00
TiO_2	1.17	2.62	0.70	1.45	0.37	1.62	1.66	1.44	1.57	1.34	0.12	0.03	0.04	0.13	0.03	0.04	0.14	0.05	1.05	1.79	1.47	1.68
Al_2O_3	13.81	1.05	0.95	16.90	16.87	11.75	11.45	9.32	12.78	12.25	3.40	1.68	1.84	3.80	1.88	2.03	3.04	2.27	16.94	16.81	16.42	17.20
Fe_2O_3	8.62	6.68	6.91	13.92	12.57	13.01	10.43	12.30	10.09	5.65	8.60	7.22	7.23	9.62	8.09	7.97	8.7	8.63	8.49	10.34	9.38	9.78
MnO	0.23	0.14	0.17	0.20	0.12	0.25	0.16	0.25	0.22	0.15	0.11	0.11	0.08	0.12	0.12	0.09	0.12	0.12	0.22	0.17	0.16	0.17
MgO	7.87	13.21	14.74	12.98	28.32	12.27	29.05	13.05	24.71	33.27	35.06	38.36	39.36	39.21	42.96	43.36	39.7	42.3	9.49	7.54	7.94	7.35
CaO	28.61	24.69	23.60	14.94	0.35	18.93	4.14	20.65	8.84	2.23	0.57	0.00	0.00	0.64	0.00	0.00	2.42	1.71	11.78	9.82	10.21	11.23
Na_2O	0.08	0.44	0.33	0.46	0.00	1.67	0.00	1.44	0.20	0.05	0.20	0.32	0.00	0.22	0.36	0.00	0.00	0.00	2.29	3.98	4.49	3.16
K_2O	0.00	0.00	0.00	0.03	0.00	0.18	0.00	0.15	0.02	0.00	0.00	0.00	0.00	0.00	0.00	0.00	0.00	0.00	0.09	0.09	0.28	0.40
P_2O_5	0.18	0.68	0.01	0.17	0.04	0.17	0.16	0.21	0.24	0.19	0.02	0.01	0.01	0.02	0.01	0.01	0.02	0.01	0.11	0.20	0.19	0.21
Cr_2O_3	0.03	0.04	0.04	0.05	0.01	0.04	0.08	0.03	0.04	0.03	0.25	0.36	0.40	0.28	0.40	0.44	0.34	0.39	0.04	0.03	0.03	0.03
NiO_2	0.01	0.02	0.02	0.04	0.05	0.03	0.07	0.02	0.03	0.03	0.34	0.19	0.40	0.38	0.21	0.44	0.31	0.36	0.02	0.02	0.02	0.01
L.O.I.	3.84	0.22	0.79	12.19	10.83	7.92	10.09	10.99	12.13	12.72	10.78	11.31	10.07	—	—	—	1.74	0.53	1.51	1.12	0.37	1.21
Σ	99.76	100.49	100.73	99.79	100.09	100.27	100.67	100.17	100.56	100.06	100.18	100.59	100.84	99.98	99.98	100.00	99.3	99.8	99.08	99.83	98.90	99.43
(ppm)																						
F	534	499	517	410	<10	331	<10	496	<10	<10	<10	<10	<10						226	218	167	
Ba	<10	22	<10	<10	<10	<10	<10	<10	<10	<10	<10	<10	<10						<10	<10	14	
Rb	<8	<8	<8	<8	<8	<8	<8	<8	<8	<8	<8	<8	<8						<8	<8	<8	
Sr	24	83	75	212	<15	44	18	45	28	<15	<15	<15	<15						173	249	348	
Pb	10	12	11	<5	<5	12	13	13	9	<5	<5	7	<5						<5	<5	<5	
Th	<5	<5	<5	<5	<5	<5	<5	<5	<5	<5	<5	<5	<5						<5	<5	<5	
U	<10	<10	<10	<10	<10	<10	<10	<10	<10	<10	<10	<10	<10						10	13	<10	
Nb	21	20	16	12	14	19	18	22	26	15	5	13	12						<10	<10	<10	
La	<20	<20	<20	<20	<20	<20	<20	<20	<20	<20	<20	<20	<20						<20	<20	<20	
Ce	<15	<15	22	23	<15	22	<15	44	<15	<15	<15	<15	<15						<15	<15	<15	
Nd	<25	<25	<25	<25	<25	<25	<25	29	<25	<25	<25	<25	<25						<25	<25	<25	
Y	31	64	36	46	12	47	35	50	96	21	3	9	7						31	47	17	
Zr	109	228	150	135	30	137	132	136	141	104	<10	15	14						79	150	122	
V	132	204	168	150	68	196	<10	299	124	<10	79	36	51						170	258	210	
Cr	194	378	336	492	<6	268	728	246	288	151	2172	2771	3372						315	210	243	
Ni	169	166	209	425	393	294	567	181	241	250	1963	1154	2457						183	154	138	
Co	78	87	78	124	109	98	39	82	78	63	91	25	83						43	164	43	
Cu	13	227	9	15	11	9	10	23	25	5	31	29	182						9	22	55	
Zn	96	62	65	83	86	100	85	86	106	56	53	59	54						90	83	57	
Ga	9	3	2	6	9	9	12	6	9	9	3	5	4						14	18	10	
Sc	4	46	55	46	13	46	44	30	43	24	16	6	14						30	41	36	
S	<50	<50	<50	<50	<50	<50	<50	<50	<50	<50	187	276	<50						<50	<50	<50	
X_{Mg}	0.50	0.69	0.70	0.51	0.71	0.51	0.76	0.54	0.73	0.87	0.82	0.86	0.86				0.83	0.84	0.55	0.45	0.48	0.46
Sp. gr.	3.33			2.82	2.75			3.01		2.72	2.68	2.65	2.72				3.18	3.21	2.96	2.96	3.00	

Table 3 Rare earth element contents of rodingites (ICP-MS). Bulk-rock compositions were determined with an ELAN 5000 and ELAN 6000 (Perkin Elmer Sciex) mass spectrometer using natural USGS reference rock samples for calibration at EMPA Dübendorf/Switzerland. The analytical uncertainties are about 2 to 7% (standard deviation 1σ). Cc–Cavloc area, Ca–Cassandra area, Si/Zo–Sissone/Zocca area.

sample	AP 9425	AP 9436	AP 9437	AP 9454	AP 9418	AP 9421	AP 9423	AP 9473	AP 9542	AP 9543	AP 9631	AP 9636	AP 9407	AP 9557	AP 9680
area	Cc	Cc	Cc	Cc	Ca	Ca	Ca	Ca	Ca	Ca	Ca	Ca	Si/Zo	Si/Zo	Si/Zo
La	10.700	10.900	7.300	3.680	15.200	4.680	6.060	14.000	5.341	3.030	8.114	3.089	10.754	3.093	7.236
Ce	32.400	35.600	23.900	9.510	39.300	12.600	13.800	37.000	13.844	8.153	19.199	9.957	33.037	9.561	14.920
Pr	4.870	5.580	3.930	1.510	5.230	1.890	1.990	4.970	1.748	1.060	2.622	1.579	5.322	1.479	1.932
Nd	24.600	29.200	20.200	7.330	24.600	9.790	9.550	23.300	7.677	5.320	11.553	6.926	25.444	6.732	8.006
Sm	7.610	9.340	6.620	2.440	6.790	3.430	2.950	6.670	2.039	1.782	3.349	2.023	6.612	2.107	2.189
Eu	2.840	3.260	2.350	1.040	2.220	1.460	1.100	2.710	0.810	0.716	1.139	0.707	1.944	0.724	0.815
Gd	9.180	11.800	8.420	3.340	8.180	4.520	3.590	8.470	2.451	2.519	4.266	2.343	6.856	2.804	2.511
Tb	1.390	1.860	1.280	0.634	1.230	0.765	0.621	1.370	0.396	0.381	0.726	0.363	1.140	0.469	0.388
Dy	8.490	11.000	7.900	3.840	7.420	4.450	3.580	8.320	2.546	2.559	5.365	2.798	6.752	3.181	2.917
Ho	1.780	2.210	1.680	0.847	1.530	0.926	0.742	1.750	0.542	0.534	1.172	0.592	1.337	0.673	0.617
Er	5.030	5.990	4.810	2.570	4.400	2.640	2.120	5.120	1.504	1.417	3.392	1.651	3.477	1.912	1.719
Tm	0.707	0.799	0.667	0.379	0.612	0.367	0.290	0.735	0.215	0.205	0.502	0.237	0.463	0.272	0.247
Yb	4.010	4.720	3.680	2.300	3.460	2.220	1.850	4.180	1.234	1.051	3.059	1.388	2.753	1.638	1.468
Lu	0.604	0.635	0.522	0.361	0.550	0.334	0.261	0.691	0.190	0.179	0.466	0.211	0.417	0.251	0.223
$(La/Yb)_N$	0.88	0.73	0.70	0.95	1.41	0.86	1.29	1.32	1.65	1.07	1.52	0.96	1.02	0.92	2.08
$(La/Sm)_N$	1.80	1.56	1.34	1.08	2.96	1.42	2.21	2.26	2.92	1.94	1.79	1.50	2.63	1.27	3.32

ume factors of 0.91 to 1.07. Assuming immobility of these elements the rodingitization can be considered as a constant volume process. In these zones TiO_2 remains immobile, whereas SiO_2 is removed by 9 g per 100 g parent rock in both localities Cassandra and Zocca. CaO is added in locality Cassandra with 21.5 g per 100 g parent rock, and in locality Zocca with 13.5 g per 100 g parent rock. FeO_{tot} has not been removed in locality Zocca, but slightly added in locality Cassandra (3 g per 100 g parent rock at a volume factor of 1). In all three localities there is a gain of an assumed H_2O-rich fluid (based upon the loss on ignition) of 0.4 to 5.3 g per 100 g parent rock (for a volume factor of 1). Assuming immobility of MgO and Al_2O_3 in locality Giumellino, a choice of a specific volume factor is difficult. This could be an effect of remobilization of these elements during the Alpine recrystallization of the rodingite assemblage (see chapter 3.1.).

The addition of CaO is reflected by the presence of calc-silicate minerals (grossular, vesuvianite, diopside and epidote) not being part of the magmatic assemblage plagioclase + clinopyroxene + olivine. The removal of alkaline elements like Na_2O reflects the disappearance of magmatic plagioclase in the rodingite. The loss of SiO_2 leads to the formation of calc-silicate minerals poorer in SiO_2 than magmatic plagioclase.

Blackwall

Inspection of some major and trace elements shows that the blackwall has TiO_2, Al_2O_3, Zr, Y, V, Ni and Cr values that are (at least for the blackwalls in locality Giumellino and Zocca) typical for basaltic rocks (see Table 2, where an average Forno metabasalt and serpentinites are given for comparison). Corresponding values of serpentinites are much lower (TiO_2, Al_2O_3, Zr, Y and V) or much higher (Ni and Cr). Thus, a basaltic origin of these altered rocks is assumed.

For a composition-volume relationship only the alteration from a metarodingite (as unaltered rock) to a chlorite blackwall (as altered rock) has been considered. All three localities display a strong enrichment of MgO and a strong depletion of CaO for the blackwalls (over a wide range of volume factors, Fig. 11). TiO_2 and Na_2O remain immobile, whereas SiO_2 is depleted. In lo-

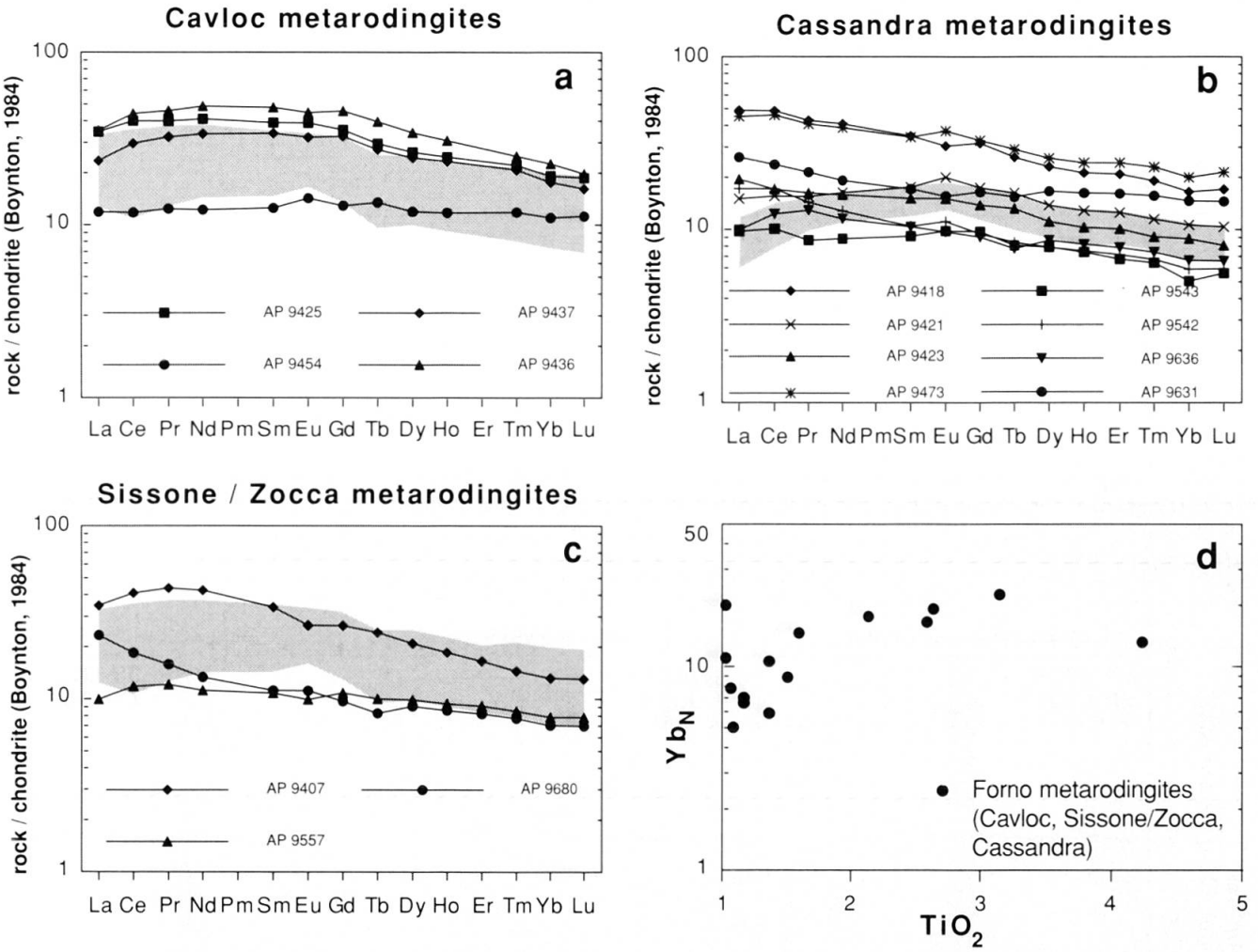

Fig. 8 REE patterns of (a) Cavloc metarodingites (in comparison with Forno metabasalts, shaded area), (b) Cassandra metarodingites (in comparison with Forno metabasalts from the Cassandra area, shaded area), and (c) Sissone metarodingites (in comparison with Forno metabasalts, shaded area). (d) Increasing REE contents with increasing differentation documented by the chondrite-normalized HREE Yb. Normalization on an average CI chondrite (BOYNTON, 1984).

calities Cassandra and Giumellino, Al_2O_3 and FeO_{tot} intercept the zero line of compositional change at a volume factor of 1 and 1.17 to 1.25, respectively. At Alpe Zocca, however, a slight depletion of FeO_{tot} and Al_2O_3 seems reasonable, because an intercept of these elements with the zero line from 1.38 to 1.86 leads to geologically unrealistic volume increase of up to 86 volume percent. A textural evidence for such a volume increase has not been observed in thin sections. In all three localities there is a gain of volatiles (based upon the loss on ignition) of 3.2 to 6.6 g per 100 g parent rock (for a volume factor of 1).

The addition of MgO is reflected by the presence of Mg-rich chlorite being Mg-richer than the chlorite in the metarodingite, the loss of CaO and SiO_2 by the disappearance of calc-silicate minerals.

3.4. Sr ISOTOPE SYSTEMATICS DURING RODINGITIZATION

$^{87}Sr/^{86}Sr$ whole rock ratios of 3 metabasalts and 5 metarodingites have been determined by W. Hansmann (Institut für Isotopengeologie und Mineralische Rohstoffe, ETH Zürich, Table 4). The $^{87}Sr/^{86}Sr$ ratios for the metabasalts and metarodingites have been recalculated to the initial $^{87}Sr/^{86}Sr$ values with the Sr and Rb contents of the analyzed rocks. Because the Rb contents of both metabasalts and metarodingites are below the detection limit (= 8 ppm) of the applied X-Ray fluorescence analysis, the initial $^{87}Sr/^{86}Sr$ ratios have been recalculated with a typical minimum and a maximum Rb content of MOR basalts (0.6 and 5 ppm, respectively; e.g. SUN, 1980; SCHILLING et al., 1983; HOFMANN, 1988; SUN and MCDONOUGH, 1989). In comparison with paleogeographic reconstructions and lithstratigraphic correlation of

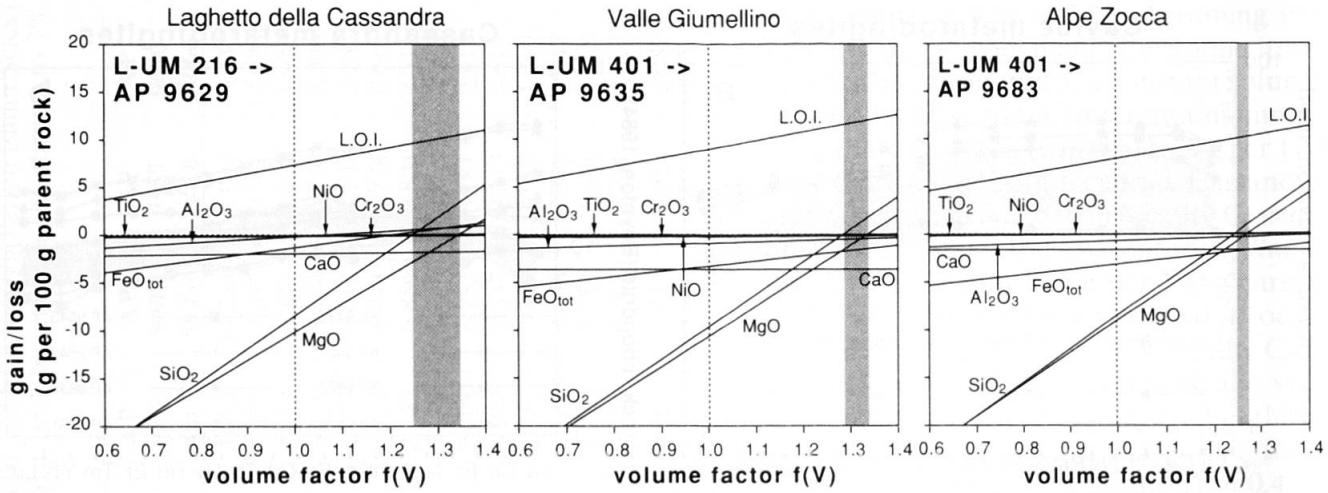

Fig. 9 Composition-volume diagrams after GRESENS (1967) for the process of serpentinization. Serpentinite AP 9629 (Laghetto della Cassandra) has been compared with the Malenco peridotite L-UM 216 (from MÜNTENER, 1997); the serpentinites AP 9635 (Valle Giumellino) and AP 9683 (Alpe Zocca) are compared with L-UM 401 (from MÜNTENER, 1997).

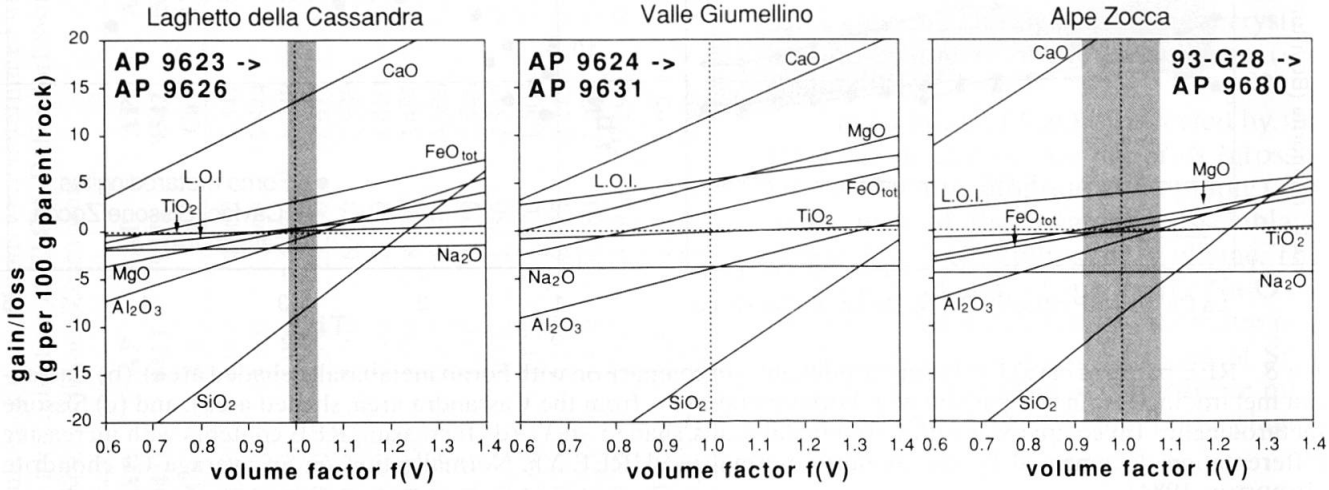

Fig. 10 Composition-volume diagrams after GRESENS (1967) for the process of rodingitization. Rodingite AP 9626 (Laghetto della Cassandra) has been compared with the Forno metabasalt AP 9623, the rodingite AP 9631 (Valle Giumellino) with AP 9624, and the rodingite AP 9680 (Alpe Zocca) with 93-G 28 (from BORSIEN, 1995).

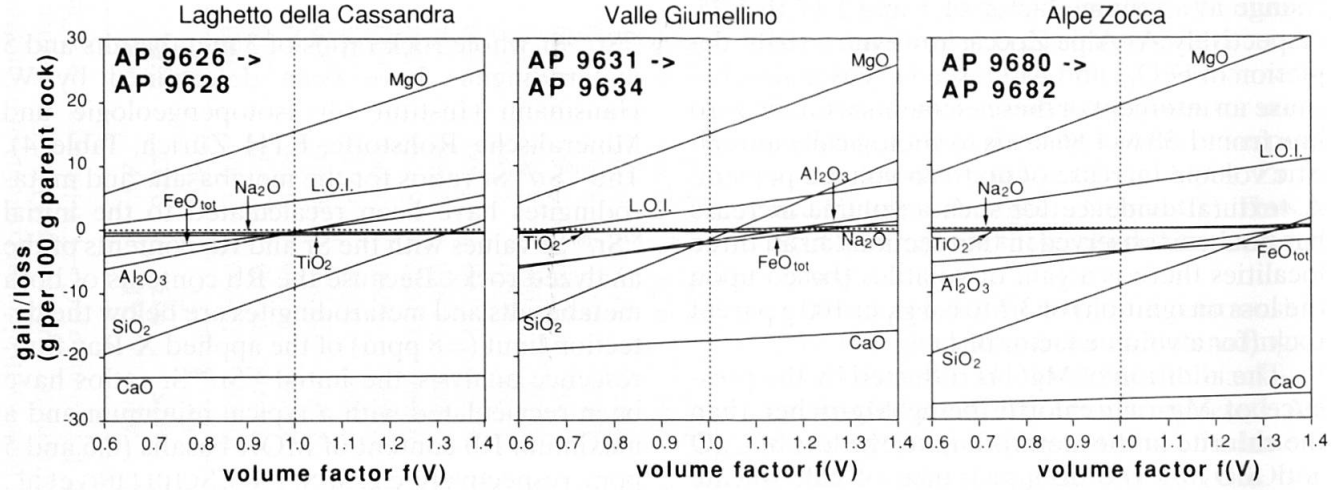

Fig. 11 Composition-volume diagrams after GRESENS (1967) for the process of blackwall formation. Chlorite blackwall AP 9628 (Laghetto della Cassandra) has been compared with the rodingite AP 9626, the chlorite blackwall AP 9634 (Valle Giumellino) with AP 9631, and the chlorite blackwall AP 9682 (Alpe Zocca) with AP 9680.

Table 4 $^{87}Sr/^{86}Sr$ determined for Forno metabasalts and metarodingites and recalculated to a range of initial ratios with t = 150 Ma and Rb(min) = 0.6 ppm and Rb(max) = 5 ppm (*). The metabasalts and metarodingites display a profile from regional metamorphic (AP 9626, AP 9631, AP 9636) to high-grade contact metamorphic overprint (AP 9623, AP 9624, AP 9680 in the olivine + tremolite stability field for ultramafic rocks; AP 9696, AP 9557 olivine + talc). Isotopic ratios of Sr for comparison: Jurassic seawater from VEIZER (1989), different MOR basalt types from SCHILLING et al. (1983) and SAUNDERS et al. (1988). Sr contents for comparison: Jurassic seawater from FAURE (1977) and VEIZER (1989), different MOR basalts from SUN (1980), SCHILLING et al. (1983), HOFMANN (1988) and SUN and MCDONOUGH (1989).

sample	$^{87}Sr / ^{86}Sr$ (measured)	Sr [ppm]	Rb [ppm]	$^{87}Sr / ^{86}Sr$ (initial)
Forno metabasalts:				
AP 9623	0.703038 ± 0.000007	173	< 8	0.702859 – 0.703016*
AP 9624	0.703501 ± 0.000016	249	< 8	0.703377 – 0.703486*
AP 9696	0.702675 ± 0.000015	168	< 8	0.702491 – 0.702652*
Forno metarodingites:				
AP 9680	0.705798 ± 0.000012	24	< 8	0.704512 – 0.705643*
AP 9626	0.704331 ± 0.000016	89	< 8	0.703984 – 0.704289*
AP 9631	0.705014 ± 0.000015	41	< 8	0.704261 – 0.704923*
AP 9636	0.705068 ± 0.000027	43	< 8	0.704350 – 0.704981*
AP 9557	0.705197 ± 0.000015	31	< 8	0.704201 – 0.705077*
For comparison:				
seawater Jurassic				0.7068 – 0.7076
seawater at 150 Ma		8		0.7069
N-MORB Atlantic				0.70229 – 0.70316
N-MORB Pacific				0.70240 – 0.70311
N-MORB Indian				0.70274 – 0.70311
T-MORB				0.7026 – 0.7031
E-MORB				0.70280 – 0.70334
average N-MORB		100		0.702725
average T-MORB		290		0.702850
average E-MORB		530		0.703070

the first sediments overlying the metavolcanics in the Piemontese Ligurian basin (WEISSERT and BERNOULLI, 1985) a Late Jurassic age (t = 150 Ma) for the basalts has been assumed and taken for the calculation.

The correction for Rb has a small influence onto the $^{87}Sr/^{86}Sr$ ratio of the metabasalts. The range of their $^{87}Sr/^{86}Sr$ initials from 0.702381 to 0.703476 overlaps with the MORB range (Fig. 12) and therefore, it appears that the metabasalts most probably preserved their primary MORB signature.

$^{87}Sr/^{86}Sr$ ratios of seawater are distinctly higher than $^{87}Sr/^{86}Sr$ ratios of mafic oceanic rocks. $^{87}Sr/^{86}Sr$ of seawater varies with time and shows a range of 0.7067 to 0.7092 for the Phanerozoic (VEIZER, 1989). Ocean floor basalts have a $^{87}Sr/^{86}Sr$ variation of 0.702 to 0.705 (FAURE, 1977). A metasomatic interaction of seawater with basaltic rocks can therefore change the $^{87}Sr/^{86}Sr$ ratio of basaltic rocks. A higher $^{87}Sr/^{86}Sr$ ratio of metarodingitic rocks compared to the $^{87}Sr/^{86}Sr$ of metabasaltic rocks may indicate a contribution of seawater to the process of rodingitization. The correction of Rb has a strong effect onto the $^{87}Sr/^{86}Sr$ of the metarodingites, leading to a large range of $^{87}Sr/^{86}Sr$ from 0.703984 to 0.705643. The $^{87}Sr/^{86}Sr$ ratios of the rodingites are significantly higher than that of the metabasalts and lie between the ratio for MOR basalts and Jurassic seawater (Fig. 12).

4. Discussion

4.1. PETROGRAPHY AND STABILITY OF RODINGITES

Two different metasomatic alteration processes can be distinguished:

(i) A rodingite formation prior to D_1 is established by the D_1 boudinage of the rodingites. The rodingitization is penetrative and static with local formation of veins and replaces probably a magmatic texture. Domains of a prekinematic equigranular assemblage in the central part of the metarodingite as well as garnet and vesuvianite veins are interpreted to represent the (oceanic) rodingite paragenesis. In metarodingites at Alpe Zocca grossular and chlorite forming long ledges most probably are pseudomorphs after magmatic plagioclase and the fine-grained chlorites and vesuvianites could represent the glassy matrix of a ba-

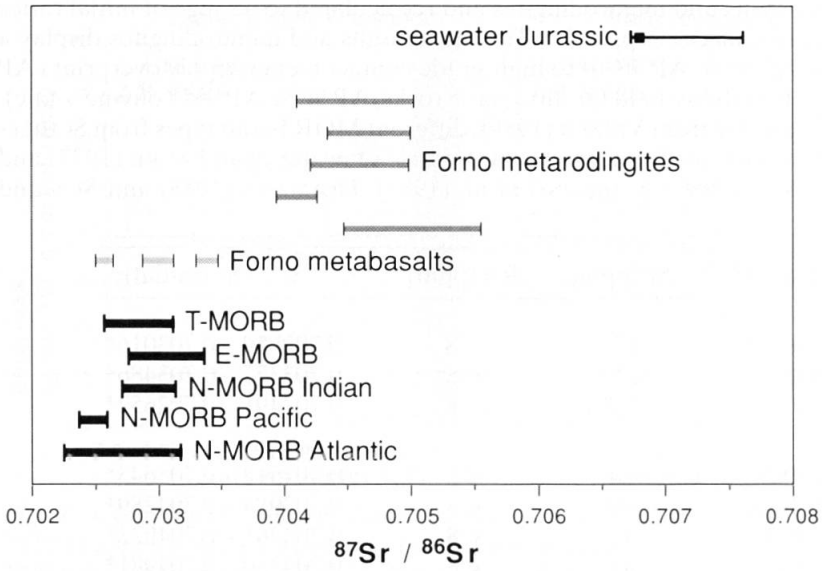

Fig. 12 $^{87}Sr/^{86}Sr$ ratios of Forno metabasalts and metarodingites from the Forno-Malenco unit compared with the ratios of Jurassic seawater (VEIZER, 1989) and MOR basalts (SAUNDERS et al., 1988; SCHILLING et al., 1983). The range of $^{87}Sr/^{86}Sr$ initials of the studied rocks are recalculated with typical Rb contents of MOR basalts.

saltic precursor. Such a magmatic texture has also been reported by RÖSLI (1988) for rodingitized diabases from the Oberhalbstein area. This process is attributed to a stage on the ocean floor.

(ii) The blackwall formation is synkinematic to D_1 and affects on a centimeter scale and irregularly the rims of the rodingitic boudins. Relics of calc-silicate minerals and garnet veins within the blackwall zones document that the blackwall overprints the rodingite. Postkinematic minerals in all lithological units most probably belong to the contact metamorphic overprint of the Bergell intrusives.

Two different ages for these metamorphic overprints can be established: An oceanic (probably Mid to Late Jurassic) age for rodingitization and an Alpine (probably Early Cretaceous) age for the blackwall formation.

The metarodingites from the study area most probably display identical mineral assemblages for both the oceanic stage and the Alpine regional metamorphic overprint (Table 1). Postkinematically grown minerals are probably contact metamorphic grown.

Stability of rodingites

Studies on rodingites with different overprint document a wide range of metamorphic conditions of the assemblage grossular + vesuvianite + chlorite ± calcite ± epidote ± diopside, e.g. from

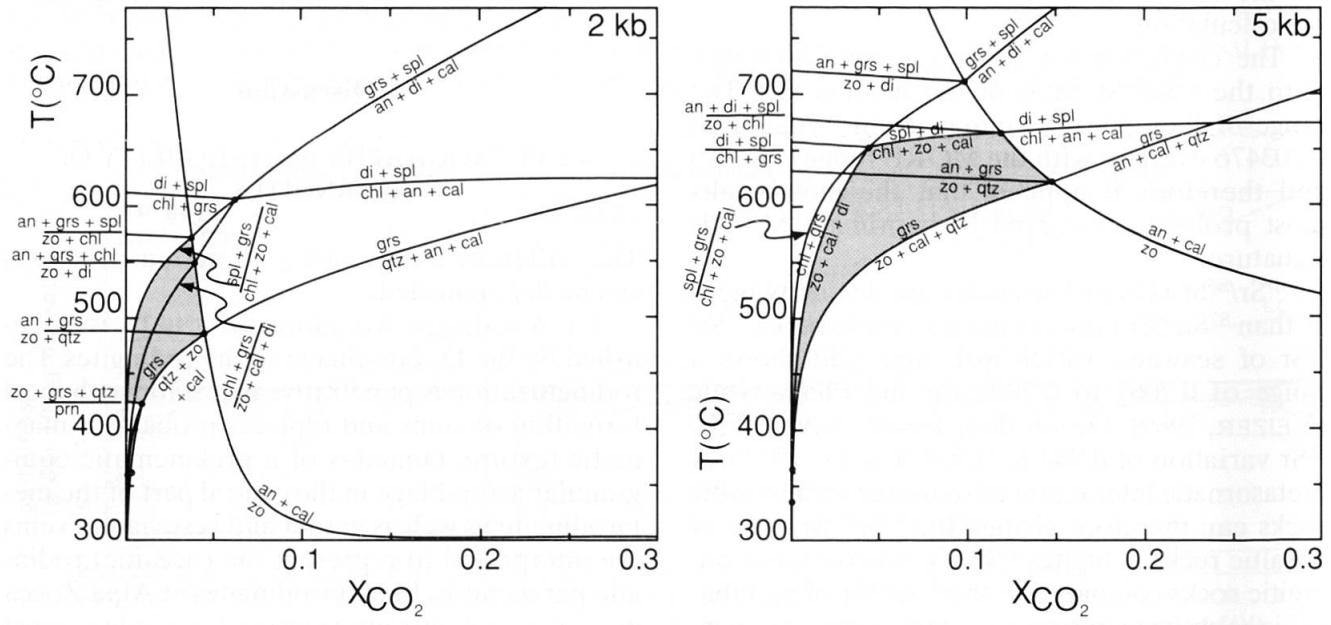

Fig. 13 H_2O-rich T–XCO_2 diagram for mixed volatile reactions in rodingites (calculated with VERTEX of CONNOLLY, 1990 and thermodynamic data from HOLLAND and POWELL, 1990). The stability field of grossular for the Forno rocks is given by the shaded area. An—anorthite, cal—calcite, chl—chlorite, di—diopside, grs—grossular, prn—prehnite, qtz—quartz, spl—spinel, zo—zoisite.

fracture zones of the Mid-Atlantic ridge (HONNOREZ and KIRST, 1975), from Liguria with prehnite-pumpellyite facies overprint (BARRIGA and FYFE, 1983; RÖSLI, 1988), and for the Oberhalbstein area with its Alpine low-grade to greenschist facies overprint (RÖSLI, 1988).

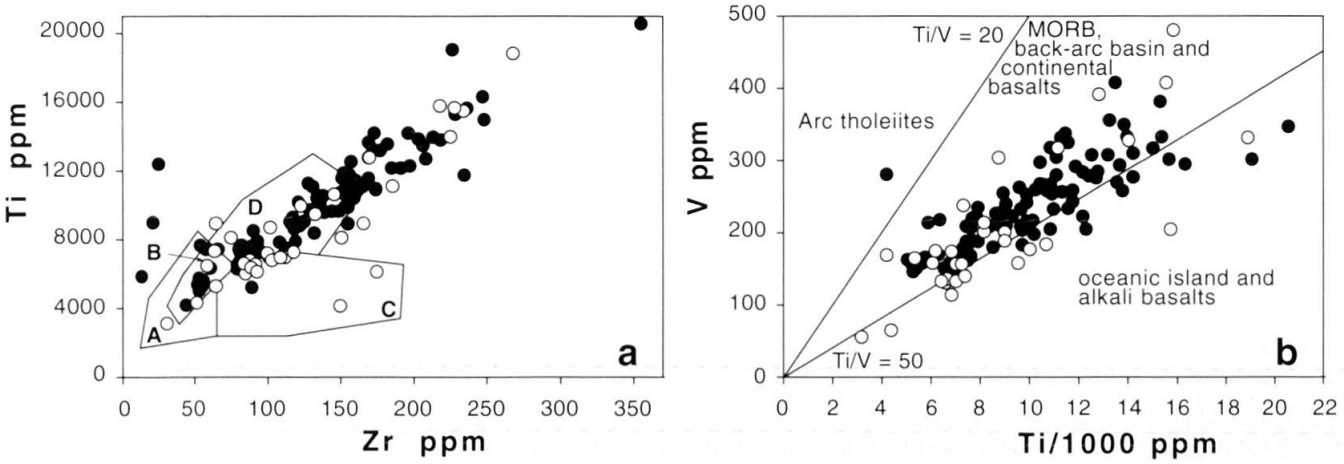

Fig. 14 Forno metabasalts and metarodingites in (a) the Ti–Zr discrimination diagram for basalts (PEARCE and CANN, 1973) and (b) the Ti–V discrimination diagram for basalts (SHERVAIS, 1982) with own data and data from GAUTSCHI (1980), KUBLI (1983), DIETHELM (1984), GIERÉ (1985), BORSIEN (1995) and PAGLIA (1996).

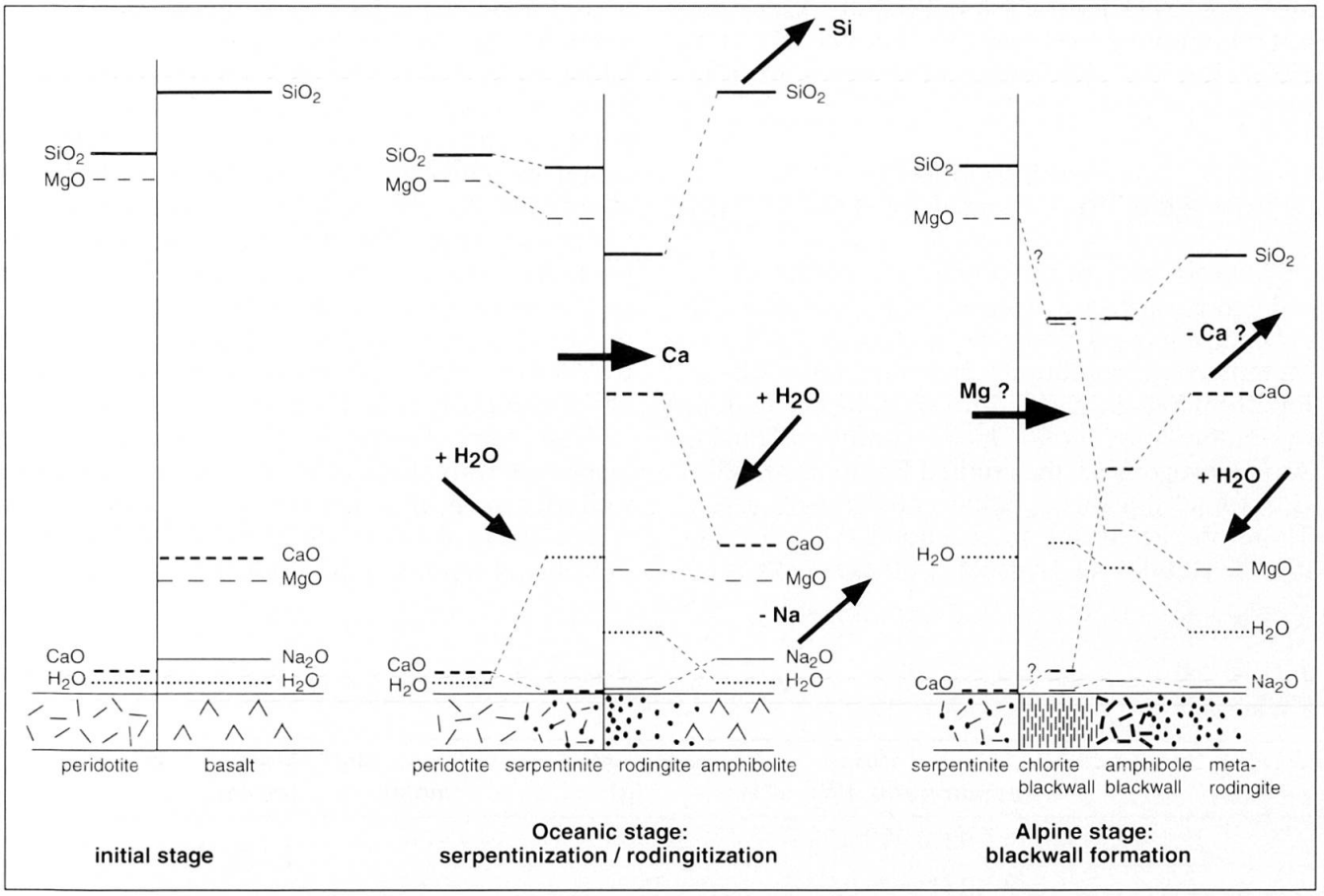

Fig. 15 Schematic sketch showing the mobility of some important major elements from the initial stage to the stage of serpentinization/rodingitization (oceanic stage) and the process of blackwall formation (Alpine stage).
Oceanic stage: The breakdown of clinopyroxene and Ca-bearing orthopyroxene during serpentinization leads to a transfer of calcium to the metabasalt and an 'uphill' enrichment in the rodingite. During serpentinization silica and sodium has been removed.
Alpine stage: Hydration and a complementary transfer of magnesia (enrichment) and calcium (decrease) leads to an Alpine alteration of the metabasaltic precursor.

The upper thermal stability of grossular + vesuvianite + chlorite in rodingites is given by the appearance of serpentine in the surrounding ultramafic rocks (FROST, 1975). Rodingites in the talc + olivine stability field have the characteristic assemblage epidote + diopside + spinel, and at higher grades plagioclase + grossular + diopside (FROST, 1975).

Mineral reactions for rodingites have been calculated in a CMASH system (RICE, 1983, Fig. 13). Typical rodingitic parageneses containing grossular, vesuvianite, chlorite, zoisite and calcite coexist with a H_2O-rich fluid composition and are bounded towards higher XCO_2 by the reaction (RICE, 1983):

$$2 \text{ zoisite} + CO_2 = 3 \text{ anorthite} + \text{calcite} + H_2O \quad (1).$$

Vesuvianite is not a diagnostic phase of metamorphism as it is stable in unmetamorphosed areas (COLEMAN, 1967) and a common phase in rodingites spanning a wide range of metamorphic grade (e.g. HONNOREZ and KIRST, 1975; BARRIGA and FYFE, 1983; RÖSLI, 1988). Prehnite disappears at temperatures between 250 and 400 °C (RICE, 1983). The first appearance of spinel is given by the reaction (RICE, 1983):

$$\text{grossular} + \text{chlorite} = 3 \text{ diopside} + 2 \text{ spinel} + 4\ H_2O \quad (2).$$

Microscopic observations of Forno metarodingites suggest a wide stability field from an oceanic stage to Alpine recrystallization (Table 1). Metamorphic conditions probably range therefore from low-grade conditions on the ocean floor to epidote-amphibolite facies conditions during Alpine orogeny. In the studied Forno metarodingites spinel and anorthite have not been observed. Therefore, according to reaction (1) (anorthite-in), the stability of grossular in these rocks is restricted in a T–XCO_2 diagram to fluids with XCO_2 less than 0.15 (for $P_{fluid} < 5$ kbars; RICE, 1983, Fig. 15). Assemblages containing grossular + chlorite are only stable at $XCO_2 < 0.04$. Reaction (2) (spinel-in) gives an upper thermal limit for the grossular stability of about 600 °C at 2 kbars and at about 650 °C at 5 kbars.

Therefore, the lack of prehnite and the presence of grossular indicates greenschist facies conditions of > 250 °C, with a very H_2O-rich fluid composition. With increasing temperature and pressure the observed Alpine metarodingitic assemblage has an upper stability of 600 to 650 °C (spinel-in). This is in accordance with the surrounding antigorite-bearing rocks in the Malenco region, that were not heated above 550 °C for variable pressures (TROMMSDORFF and CONNOLLY, 1996).

Blackwall formation

The formation of blackwalls results most probably from Alpine prograde reactions that supply volatiles, sodium and magnesia from the surrounding rocks. Possible reactions leading to the mobilization of these elements are continuous reactions of albite to oligoclase (sodium) in neighbouring crystalline rocks and the breakdown of brucite (magnesia and volatiles) in serpentinites. A lower temperature limit for the blackwall formation is the reaction of antigorite and brucite to forsterite at about 400 °C (brucite-out, TROMMSDORFF and CONNOLLY, 1996). The surrounding antigorite serpentinites give an upper temperature limit, where antigorite would break down to olivine + talc approximately at 500 to 550 °C (TROMMSDORFF and CONNOLLY, 1996). This breakdown, however, was never encountered at the studied localities.

This temperature bracket for the Alpine blackwall formation (400 to 550 °C) coincides well with the peak temperature estimates of HERMANN (1997) of 450 to 500 °C for the Alpine metamorphic overprint in the studied area.

Table 5 Recalculation of gain and loss of MgO and CaO of the blackwall formation onto a molar Mg^{2+}/Ca^{2+} ratio assuming no volume change (f(V) = 1).

locality	gain/loss (assumption f(V) = 1)	recalculated as Ca^{2+} and Mg^{2+} [g]	[mole]	Mg^{2+}/Ca^{2+} ratio [molar]
Cassandra	15.4 g per 100 g MgO	9.29	0.38	0.93
	–23.1 g per 100 g CaO	–16.5	0.41	
Giumellino	15.0 g per 100 g MgO	9.05	0.37	1.19
	–17.5 g per 100 g CaO	–12.5	0.31	
Alpe Zocca	19.3 g per 100 g MgO	11.6	0.48	1.00
	–26.8 g per 100 g CaO	–19.2	0.48	

4.2. WHOLE ROCK CHEMISTRY

Based upon main, trace elements and REE a basaltic origin for the rodingitic rocks can be established. During rodingitization the basaltic precursor lost SiO_2. This is documented by the shift of the bulk-rock values of the rodingites towards the rodingitic model phases (with the exception of diopside and tremolite) that have lower SiO_2 contents than the predominant magmatic model phase plagioclase. The Na_2O depletion with increasing CaO content is typical for rodingites and reported by several authors (e.g. EVANS et al., 1979; PUGA et al., 1999).

The contents of Ti, Zr and V in the rodingites are not markably different with respect to the metabasalts, and the REE patterns are similar to that of the metabasalts (Fig. 8), indicating that rodingitization has not severly mobilized these elements. The immobility of the high field strength elements permits the use of discrimination diagrams originally developed for basalts also for the studied Forno rocks (e.g. Ti–Zr diagram of PEARCE and CANN, 1973, Ti–V diagram of SHERVAIS, 1982; Fig. 14). The REE patterns of the metabasalts support a low-pressure fractionation of the assemblage plagioclase + olivine + clinopyroxene for the Forno unit (PUSCHNIG, 2000) typical for ocean floor basalts (e.g. SCHILLING et al., 1983).

4.3. Sr ISOTOPES

The metarodingites display a profile from regional metamorphic to high-grade contact metamorphic overprint, where $^{87}Sr/^{86}Sr$ do not change systematically. Therefore the influence of regional and contact metamorphism onto the $^{87}Sr/^{86}Sr$ of metabasalts and metarodingites may be very small.

Most of the MOR basalts and tholeiites from different regions show only minor variation in their initial $^{87}Sr/^{86}Sr$ (O'NIONS et al., 1976; EABY et al., 1984; HAMELIN et al., 1984; ITO et al., 1987). This ratio may be enriched by small seawater interaction up to 0.70377 in the upper part of the oceanic crust (BARRETT and FRIEDRICHSEN, 1982). The Forno metabasalts display a scatter from 0.702381 to 0.703476, which is slightly higher than that for fresh MOR basalts, perhaps due to a limited interaction with seawater.

The $^{87}Sr/^{86}Sr$ ratio of the metarodingites is higher than the $^{87}Sr/^{86}Sr$ ratio of both the Forno metabasalts and MOR basalts, but smaller than the $^{87}Sr/^{86}Sr$ variation of Jurassic seawater (Fig. 12). Therefore the metarodingites do not show any longer their primary magmatic signature. The increase of $^{87}Sr/^{86}Sr$ of the metarodingites with respect to the metabasalts and the MOR basalts most probably results from a strong interaction with seawater, but a magmatic interaction with a crustal component cannot be excluded. A change of $^{87}Sr/^{86}Sr$ to higher ratios for metarodingites relative to their protoliths from Lanzo and Liguria has been reported by RÖSLI (1988) and also been attributed to seawater interaction.

4.4. MASS BALANCE CALCULATION

Oxygen-based and magnesia and silica conserving model reactions for serpentinization like

$$\text{olivine} + \text{enstatite} + 2\,H_2O = \text{serpentine} \quad (3)$$
$$Mg_2SiO_4 + MgSiO_3 + 2\,H_2O = Mg_3Si_2O_5(OH)_4$$

and

$$2\,\text{olivine} + 3\,H_2O = \text{serpentine} + \text{brucite} \quad (4)$$
$$2\,Mg_2SiO_4 + 2\,H_2O = Mg_3Si_2O_5(OH)_4 + Mg(OH)_2$$

with the molar volume of forsterite of 43.79 cm^3, enstatite of 31.47 cm^3, serpentine (chrysotile) and brucite of 24.63 cm^3 (ROBIE et al., 1979) yield a volume increase for solids of 44% (3) and 52% (4), respectively. The estimated volume increase of 24 to 34% due to the serpentinization process (as deduced by Gresens diagrams) is in accordance with observations and calculations of PETERS (1963, +15%), SCAMBELLURI and RAMPONE (1999, +20%), HOSTETLER et al. (1966, +35 to 40%), RÖSLI (1988, +39%), whereas GRESENS (1967) reports volume factors of 0.67 to 1.3 for the serpentinization.

The estimation of a near volume-constant rodingitization process is in accordance with petrographic observations (preservation of the volcanic texture, Fig. 3b, no strong fractured rocks on a microscopic scale) and with calculations of SCHANDL et al. (1989), who reported a volume factor of 1.02 for a rodingitized lamprophyre. An oxygen-based model reaction for rodingitization involving the replacement of magmatic plagioclase (An_{60}) to grossular, can be written as:

$$5\,\text{anorthite}_{60} + 9\,CaO\ (\text{introduced}) = 4\,\text{grossular} + Na_2O\ (\text{removed}) \quad (5)$$
$$5\,Na_{0.4}Ca_{0.6}Al_{1.6}Si_{2.4}O_8 + 9\,CaO = 4\,Ca_3Al_2Si_3O_{12} + Na_2O$$

and, with the molar volumes of 100.07 cm^3 (albite) or 100.79 cm^3 (anorthite) for plagioclase and the molar volume of 125.3 cm^3 for grossular (ROBIE et al., 1979), yields a constant-volume rodingitization. This is consistent with calculations from the Gresens diagrams.

The process of chlorite blackwall formation is characterized by the uptake of MgO and loss of CaO, which can be described as $Mg_{+1}Ca_{-1}$ metasomatism. A recalculation of the gain of MgO and the loss of CaO, assuming a volume factor of 1, gives values of 0.927 to 1.192 for a molar Mg^{2+}/Ca^{2+} ratio (see Table 5). This coincides with an empirically and experimentally determined molar exchange of Mg^{2+} and Ca^{2+} on a 1:1 basis for hydrothermally altered basalts (HUMPHRIS and THOMPSON, 1978; MOTTL, 1983).

The gain of volatiles and MgO in both blackwall types and the high content of Na_2O in the amphibole blackwall are probably the result of the Alpine prograde regional metamorphism. Dehydration reactions in surrounding crystalline rocks and serpentinized ultramafic rocks may lead to hydration of the rodingite-serpentinite contacts and to the formation of the blackwall. A possible source for MgO is provided by the breakdown of Mg-rich phases in serpentinites such as brucite (SNOW and DICK, 1995).

Serpentinization and rodingitization are complementary processes (Fig. 15): CaO is depleted in the peridotite and concentrated in the basaltic rock which already has a much higher CaO content than the peridotite. The 'uphill' enrichment is documented by a concentration increase from approximately 10 wt% CaO in the basaltic precursor to 30 wt% CaO, accompanied by the complete loss of CaO in the peridotitic precursor (approximately 1 to 3 wt%). The rodingitization may be interpreted as a one-way infiltration process by Ca-rich aqueous solutions due to serpentinization. The subsequent blackwall formation leads to decreasing difference of the major element concentrations (e.g. CaO and MgO) of altered rocks (serpentinite and rodingite). It shifts the bulk-rock composition of the metarodingite towards the bulk-rock composition of the serpentinite (Fig. 15), which remains unaffected by this alteration. The blackwall formation has an effect of blurring, i.e. a concentration hiatus inherited from the oceanic alteration process is overprinted by the Alpine alteration resulting in smoothed concentration profiles. Similar observations have been made by SCHANDL et al. (1989). This process may be driven by diffusion between the exchanging systems in presence of a fluid.

5. Conclusions

– Two major metasomatic processes, rodingitization and blackwall formation, affected the Forno metabasalts in contact with ultramafic rocks. These processes are distinct in mechanism, metamorphic conditions and time: rodingitization (accompanying serpentinization) is an oceanic alteration process, whereas the blackwall formation is an Alpine alteration process.

– If rodingitization is considered as a constant-volume process, it can be interpreted as a one-way infiltration, on a meter scale, by Ca-rich aqueous solutions derived from the contemporaneous serpentinization (CaO increase, decrease of SiO_2 and Na_2O). Trace elements such as Ti, Zr and V and the patterns of the REE of the studied rocks do not change significantly during oceanic alteration. The patterns show the same shape as the Forno metabasalts and therefore preserved their MORB-type character.

– Forno metabasalts have $^{87}Sr/^{86}Sr$ ratios comparable with MOR basalts. Metarodingites have distinctly higher $^{87}Sr/^{86}Sr$ ratios. The increase of $^{87}Sr/^{86}Sr$ in metarodingites with respect to the adjacent metabasalts and to MOR basalts most probably results from the interaction with seawater.

– The process of chlorite blackwall formation is interpreted as a diffusive exchange on a centimeter scale, characterized by hydration and enrichment of MgO and depletion of CaO on a 1:1 molar basis ($Mg_{+1}Ca_{-1}$ metasomatism) at constant volume affecting only the metabasaltic precursor.

– Metamorphic conditions of serpentinization and rodingitization on the ocean floor most probably never exceeded approximately 500 °C at low pressures. Metamorphic conditions of the blackwall formation and the Alpine recrystallization of the rodingitic assemblage occurred in the temperature range of 400 to 550 °C.

Acknowledgements

This work was supported by the Swiss National Science Foundation (grants. No. 2000-037388.93/1 and 2000-042988.95/1). I am indepted to W. Hansmann (†) for determining the Sr isotopes and to O. Müntener and P. Ulmer for fruitful discussions and critical reading of an earlier version of the manuscript. This paper benefitted from careful reviews and helpful criticism by R. Gieré and M. Engi, which is greatly appreciated.

References

BARRETT, T.J. and FRIEDRICHSEN, H. (1982): Strontium and oxygen isotopic composition of some basalts from Hole 504B, Costa Rica Rift, DSDP Legs 69 and 70. Earth Planet. Sci. Lett. 60, 27–38.

BARRIGA, F. and FYFE, W.S. (1983): Development of rodingite in basaltic rocks in serpentinite, East Liguria, Italy. Contrib. Mineral. Petrol. 84, 146–151.

BORSIEN, G.R. (1995): Petrographische Untersuchungen im oberen Val Malenco (Val Ventina, N-Italien). Teil 1. Unpubl. diploma thesis ETH Zürich.

BOYNTON, W.V. (1984): Geochemistry of the rare earth elements: meteorite studies. In: HENDERSON, P. (ed.):

Rare earth element geochemistry. Development in Geochemistry 2. Elsevier, Amsterdam, 63–114.

BURKHARD, D.J.M. and O'NEIL, J.R. (1988): Contrasting serpentinization processes in the eastern Central Alps. Contrib. Mineral. Petrol. 99, 498–506.

COLEMAN, R.G. (1967): Low-temperature reaction zones and Alpine ultramafic rocks of California, Oregon and Washington. U.S. Geol. Surv. Bull. 1247, 1–49.

COLEMAN, R.G. (1977): Ophiolites. Springer Berlin.

CONNOLLY, J.A.D. (1990): Calculation of multivariable phase diagrams: An algorithm based on generalized thermodynamics. Am. J. Sci. 290, 666–718.

DEUTSCH, A. (1983): Datierungen an Alkaliamphibolen und Stilpnomelan der südlichen Platta-Decke (Graubünden). Eclogae geol. Helv. 76, 295–308.

DIETHELM, K.H. (1984): Geologie und Petrographie des Bergell-Ostrandes II. Unpubl. diploma thesis ETH Zürich.

EABY, J., CLAQUE, D.A. and DELANEY, J.R. (1984): Sr isotopic variation along the Juan de Fuca Ridge. J. Geophys. Res. 89, 7883–7890.

EVANS, B.W. and TROMMSDORFF, V. (1970): Regional metamorphism of ultramafic rocks in the Central Alps: parageneses in the system CaO–MgO–SiO_2–H_2O. Schweiz. Mineral. Petrogr. Mitt. 50, 481–492.

EVANS, B.W., TROMMSDORFF, V. and GOLE, G.G. (1981): Geochemistry of high-grade eclogites and metarodingites from the Central Alps. Contrib. Mineral. Petrol. 76, 301–311.

EVANS, B.W., TROMMSDORFF, V. and RICHTER, W. (1979): Petrology of an eclogite-metarodingite suite at Cima di Gagnone, Ticino, Switzerland. Am. Mineral. 64, 15–31.

FAURE, G. (1977): Principles of Isotope Geology. 2nd edition, Wiley & Son, New York.

FREY, M., HUNZIKER, J., FRANK, W., BOCQUET, J., DAL PIAZ, G.V., JÄGER, E. and NIGGLI, E. (1974): Alpine metamorphism of the Alps. A review. Schweiz. Mineral. Petrogr. Mitt. 54, 247–290.

FROITZHEIM, N., SCHMID, S.M. and CONTI, P. (1994): Repeated change from crustal shortening to orogen-parallel extension in the Austroalpine units of Graubünden. Eclogae geol. Helv. 87, 559–612.

FROST, B.R. (1975): Contact metamorphism of serpentinite, chlorite blackwall and rodingite at Paddy-Go-Easy Pass, Central Cascades, Washington. J. Petrol. 16, 272–313.

GAUTSCHI, A. (1980): Metamorphose und Geochemie der basischen Gesteine des Bergeller Ostrandes (Graubünden, Schweiz / Provinz Sondrio, Norditalien). Unpubl. Ph.D thesis ETH Zürich Nr. 6672.

GIERÉ, R. (1985): Metasedimente der Suretta-Decke am Ost- und Südostrand der Bergeller Intrusion: Lithostratigraphische Korrelation und Metamorphose. Schweiz. Mineral. Petrogr. Mitt. 65, 57–78.

GRESENS, R.L. (1967): Composition-volume relationships of metasomatism. Chem. Geol. 2, 47–65.

HAMELIN, B., DUPRÉ, B. and ALLÈGRE, C.J. (1984): Lead-strontium variations along the East Pacific Rise and the Mid-Atlantic Ridge: a comparative study. Earth Planet. Sci. Lett. 67, 340–350.

HANDY, M.R., HERWEGH, M., KAMBER, B.S., TIETZ, R. and VILLA, I. (1996): Geochronologic, petrologic and kinematic constraints on the evolution of the Err-Platta boundary, part of a fossil continent ocean suture in the Alps (eastern Switzerland). Schweiz. Mineral. Petrogr. Mitt. 76, 453–474.

HERMANN, J. (1997): The Braccia gabbro (Malenco, Alps): Permian intrusion at the crust to mantle interface and Jurassic exhumation during rifting. Unpubl. Ph.D. thesis ETH Zürich No. 12102.

HOFMANN, A.W. (1988): Chemical differentiation of the Earth: the relationship between mantle, continental crust, and oceanic crust. Earth Planet. Sci. Lett. 90, 297–314.

HOLLAND, T.J.B. and POWELL, R. (1990): An enlarged and updated internally consistent dataset with uncertainties and correlations. J. Metamorphic Geol. 8, 89–124.

HONNOREZ, J. and KIRST, P. (1975): Petrology of rodingites from the equatorial Mid-Atlantic Fracture Zones and their geotectonic significance. Contrib. Mineral. Petrol. 49, 233–257.

HOSTETLER, P.B., COLEMAN, R.G., MUMPTON, F.A. and EVANS, B.W. (1966): Brucite in Alpine serpentinites. Am. Mineral. 51, 75–98.

HUMPHRIS, S.E. and THOMPSON, G. (1978): Hydrothermal alteration of oceanic basalts by seawater. Geochim. Cosmochim. Acta 42, 107–125.

ITO, E., WHITE, W.M. and GÖPEL, C. (1987): The O, Sr, Nd and Pb isotope geochemistry of MORB. Chem. Geol. 62, 157–176.

JÄGER, E. (1973): Die alpine Orogenese im Lichte radiometrischer Altersbestimmungen. Eclogae geol. Helv. 66, 11–21.

KEUSEN, H.-R. (1972): Mineralogie und Petrographie des metamorphen Ultramafitit-Komplexes vom Geisspfad (Penninische Alpen). Schweiz. Mineral. Petrogr. Mitt. 72, 385–478.

KUBLI, Th. (1983): Geologie und Petrographie der Fornoserie im unteren Val Forno. Unpubl. diploma thesis ETH Zürich.

MONTRASIO, A. (1973): Strutture a pillow nelle anfiboliti del M. Forno (Penninico medio-Alpi Retichi). Rend. Accad. Naz. Lincei, Cl. Sci. Fis. Mat. Nat. 54, 114–123.

MONTRASIO, A. and TROMMSDORFF, V. (1983): Guida all'escursione del Massiccio di Val Masino-Bregaglia, Val Malenco Occidentale, Sondrio (Chiareggio, 16–18 luglio 1983). Mem. Soc. Geol. It. 26, 421–434.

MOTTL, M.J. (1983): Metabasalts, axial hot springs, and the structure of hydrothermal systems at mid-ocean ridges. Geol. Soc. Am. Bull. 94, 161–180.

MÜNTENER, O. (1997): The Malenco peridotites (Alps): Petrology and geochemistry of subcontinental mantle and Jurassic exhumation during rifting. Unpubl. Ph.D. thesis ETH Zürich No. 12103.

MÜNTENER, O. and HERMANN, J. (1996): The Malenco lower crust-mantle complex and its field relations. Schweiz. Mineral. Petrogr. Mitt. 76, 475–500.

O'NIONS, R.K., PANKHURST, R.J. and GRONVOLD, K. (1976): Nature and development of basalt magma sources beneath Iceland and the Reykjanes Ridge. J. Petrol. 17, 315–338.

PAGLIA, CH. (1996): Ricerche strutturali e petrografiche lungo il marchine meridionale del corpo ultramafiche del Malenco. Parte 1: Zona Cassandra (Valle Airale, Prov. Sondrio, Nord-Italia). Unpubl. diploma thesis ETH Zürich.

PEARCE, J.A. and CANN, J.R. (1973): Tectonic setting of basic volcanic rocks determined using trace elements. Earth Planet. Sci. Lett. 19, 290–300.

PERETTI, A. and KÖPPEL, V. (1986): Geochemical and lead isotope evidence for a mid-ocean ridge type mineralization within a polymetamorphic ophiolite complex (Monte del Forno, North Italy / Switzerland). Earth Planet. Sci. Lett. 80, 252–264.

PETERS, TJ. (1963): Mineralogie und Petrographie des Totalpserpentins bei Davos. Schweiz. Mineral. Petrogr. Mitt. 43, 529–685.

PFIFFNER, M. (1999): Genese der hochdruckmetamorphen ozeanischen Abfolge der Cima-Lunga-Einheit

(Zentralalpen). Unpubl. Ph.D. thesis ETH Zürich No. 13011.

PFIFFNER, M. and WEISS, M. (1994): Strukturelle und petrographische Untersuchungen im Grenzbereich Penninikum-Unterostalpin am Südostrand des Bergell-Plutons (Val Masino, Italien). Schweiz. Mineral. Petrogr. Mitt. 74, 245–264.

PHILIPP, R. (1982): Die Alkaliamphibole der Platta-Decke zwischen Silsersee und Lunghinpass (Graubünden). Schweiz. Mineral. Petrogr. Mitt. 62, 437–455.

POZZORINI, D. and FRÜH-GREEN, G. (1996): Stable isotope systematics of the Ventina ophicarbonate zone, Bergell contact aureole. Schweiz. Mineral. Petrogr. Mitt. 76, 549–564.

PUGA, E., NIETO, J.M., DÍAZ DE FEDERICO, A., BODINIER, J.L. and MORTEN, L. (1999): Petrology and metamorphic evolution of ultramafic rocks and dolerite dykes of the Betic Ophiolitic Association (Mulhacén Complex, SE Spain): evidence of eo-Alpine subduction following an ocean-floor metasomatic process. Lithos 49, 23–56.

PUSCHNIG, A.R. (1996): Regional and emplacement-related structures at the northeastern border of the Bergell intrusion (Monte del Forno, Rhetic Alps). Schweiz. Mineral. Petrogr. Mitt. 76, 399–420.

PUSCHNIG, A.R. (1998): The Forno unit (Rhetic Alps): Evolution of an ocean floor sequence from rifting to Alpine orogeny. Unpubl. Ph.D. thesis ETH Zürich No. 12702.

PUSCHNIG, A.R. (2000): The oceanic Forno unit (Rhetic Alps): field relations, geochemistry and paleogeographic setting. Eclogae geol. Helv.93, 103–124.

RICE, J.M. (1983): Metamorphism of rodingites: Part I. Phase relations in a portion of the system CaO–MgO–Al_2O_3–SiO_2–CO_2–H_2O. Am. J. Sci. 283-A, 121–150.

ROBIE, R.A., HEMINGWAY, B.S. and FISHER, J.R. (1979): Thermodynamic properties of minerals and related substances at 298.15 K and 1 Bar (10^5 Pascals) pressure and at high temperatures. U.S. Geological Survey Bull 1452.

RÖSLI, U.E. (1988): Geochemische und mineralogische Untersuchungen an Metarodingiten. Unpubl. Ph.D. thesis ETH Zürich No. 8589.

SAUNDERS, A.D., NORRY, M.J. and TARNEY, J. (1988): Origin of MORB and chemically depleted mantle reservoirs: trace elements constraints. J. Petrol., Special Lithosphere Issue, 415–445.

SCAMBELLURI, M. and RAMPONE E. (1999): Mg-metasomatism of oceanic gabbros and its control on Ti-clinohumite formation during eclogitization. Contrib. Mineral. Petrol. 135, 1–17.

SCHANDL, E.S., O'HANLEY, D.S. and WICKS, F.J. (1989): Rodingites in serpentinized ultramafic rocks of the Abitibi greenstone belt, Ontario. Can. Mineral. 27, 579–591.

SCHILLING, J.-G., ZAJAC, M., EVANS, R., JOHNSON, T., WHITE, W., DEVINE, J.D. and KINGSLEY, R. (1983): Petrologic and geochemical variations along the Mid-Atlantic Ridge from 29°N to 73°N. Am. J. Sc. 283, 510–586.

SCHMID, S.M., RÜCK, P. and SCHREURS, G. (1990): The significance of the Schams nappes for the reconstruction of the paleotectonic and orogenic evolution of the Penninic zone along the NFP-20 East traverse (Grisons, eastern Switzerland). In: ROURE, F., HEITZMANN, P., POLINO, R. (eds): Deep structure of the Alps. Mém. Soc. géol. Fr. 156; Mém. Soc. géol. suisse 1; Vol. spec. Soc. Geol. It. 1, 263–287.

SHERVAIS, J.W. (1982): Ti–V plots and the petrogenesis of modern and ophiolitic lavas. Earth Planet. Sci. Lett. 59, 101–118.

SNOW, J.E. and DICK, H.J.B. (1995): Pervasive magnesium loss by marine weathering of peridotite. Geochim. Cosmochim. Acta 59, 4219–4235.

SUN, S.-S. (1980): Lead isotope study of young volcanic rocks from mid-ocean ridges, ocean islands and island arcs. Phil. Trans. R. Soc. London A 297, 409–445.

SUN, S.-S. and MCDONOUGH, W.F. (1989): Chemical and isotopic systematics of oceanic basalts: implications for mantle composition and processes. In: SAUNDERS, A.D. and NORRY, M.J. (eds): Magmatism in ocean basins. Geol. Soc. London Spec. Publ. 42, 313–345.

TROMMSDORFF, V. and CONNOLLY, J.A.D. (1996): The ultramafic contact aureole about the Bregaglia (Bergell) Tonalite: Isotherms and a thermal model. Schweiz. Mineral. Petrogr. Mitt. 76, 537–548.

TROMMSDORFF, V. and EVANS, B.W. (1972): Progressive metamorphism of antigorite schist in the Bergell tonalite aureole (Italy). Am. J. Sci. 272, 423–437.

TROMMSDORFF, V. and EVANS, B.W. (1977): Antigorite ophicarbonates: contact metamorphism in Val Malenco. Contrib. Mineral. Petrol. 62, 301–312.

TROMMSDORFF, V. and NIEVERGELT, P. (1983): The Bregaglia (Bergell) Iorio Intrusive and its field relations. Mem. Soc. Geol. It. 26, 55–68.

TROMMSDORFF, V., PICCARDO, G.B. and MONTRASIO, A. (1993): From magmatism to sea floor emplacement of subcontinental Adria lithosphere during pre-Alpine rifting (Malenco, Italy). Schweiz. Mineral. Petrogr. Mitt. 73, 191–204.

ULRICH, T. and BORSIEN, G.R. (1996): Chemische Untersuchungen am Fedozer Metagabbro und ein Vergleich mit dem Forno Metabasalt. Schweiz. Mineral. Petrogr. Mitt, 76, 521–536.

VEIZER, J. (1989): Strontium isotopes in seawater through time. Ann. Rev. Earth Planet. Sci. 17, 141–167.

WEISSERT, H.J. and BERNOULLI, D. (1985): A transform margin in the Mesozoic Tethys: Evidence from the Swiss Alps. Geol. Rundschau 74, 665–679.

WIDMER, T. (1996): Entwässerung ozeanisch alterierter Basalte in Subduktionszonen (Zone von Zermatt-Saas Fee). Unpubl. Ph.D. thesis ETH Zürich No. 11609.

Manuscript received October 30, 2001; revision accepted September 20, 2002.
Editorial handling: M. Engi